NOL TECHNICAL REPORT

RELAXATION BEHIND STRONG SHOCK WAVES IN AIR

BY
J. M. Ward

1 October 1974

NAVAL ORDNANCE LABORATORY
WHITE OAK, SILVER SPRING, MARYLAND 20910

● Unlimited distribution; approved for public release

NAVAL ORDNANCE LABORATORY
WHITE OAK, SILVER SPRING, MARYLAND 20910
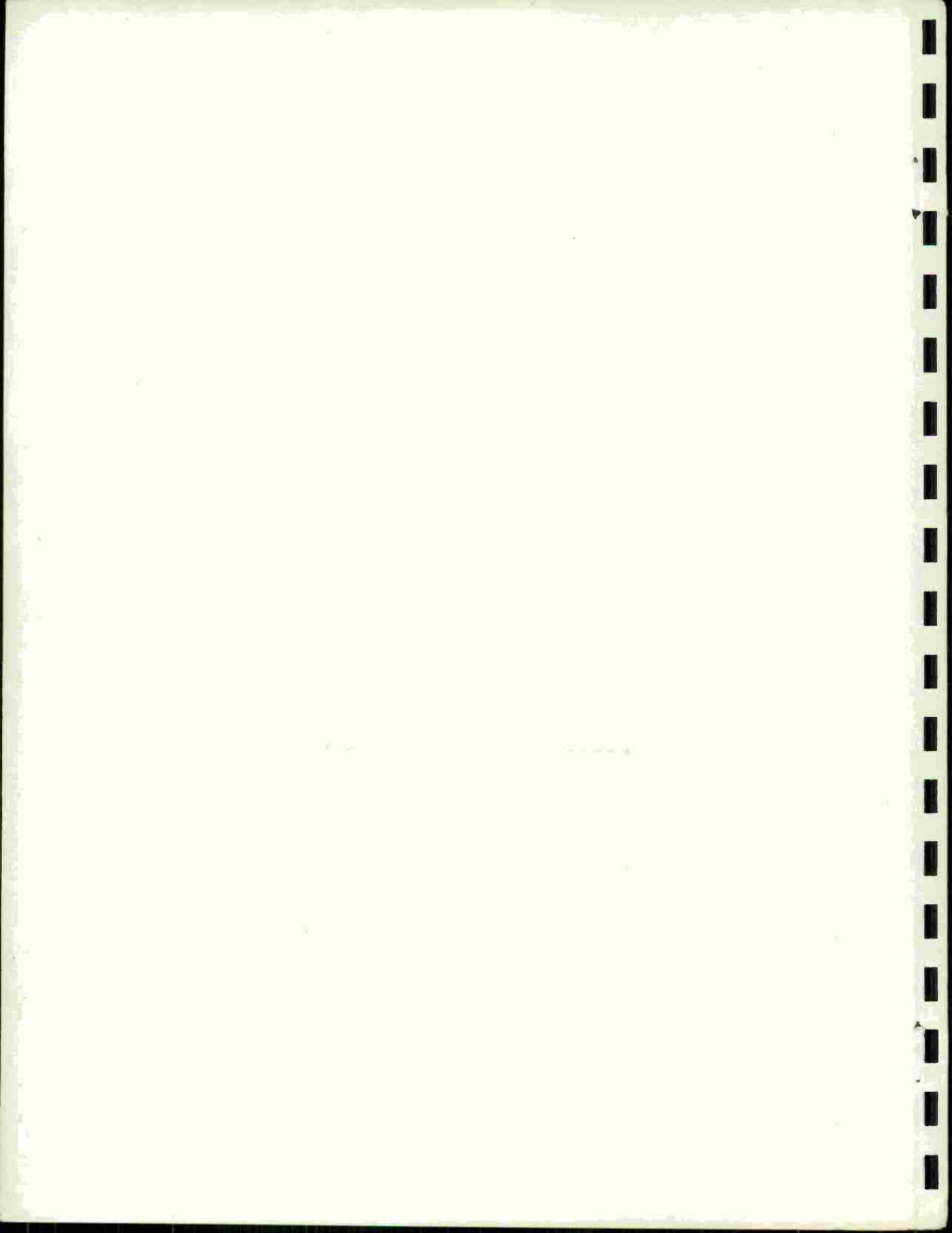
REPORT DOCUMENTATION PAGE		READ INSTRUCTIONS BEFORE COMPLETING FORM
1. REPORT NUMBER NOLTR 74-182	2. GOVT ACCESSION NO.	3. RECIPIENT'S CATALOG NUMBER
4. TITLE *(and Subtitle)* Relaxation Behind Strong Shock Waves in Air		5. TYPE OF REPORT & PERIOD COVERED Jul 72 - Jun 74
		6. PERFORMING ORG. REPORT NUMBER
7. AUTHOR(s) J. M. Ward		8. CONTRACT OR GRANT NUMBER(s)
9. PERFORMING ORGANIZATION NAME AND ADDRESS Naval Surface Weapons Center White Oak, Silver Spring, Maryland 20910 (Formerly Naval Ordnance Laboratory)		10. PROGRAM ELEMENT, PROJECT, TASK AREA & WORK UNIT NUMBERS 61152N, ZR00001 ZR00001010 MAT03L00010324
11. CONTROLLING OFFICE NAME AND ADDRESS		12. REPORT DATE 1 October 1974
		13. NUMBER OF PAGES 63
14. MONITORING AGENCY NAME & ADDRESS *(if different from Controlling Office)*		15. SECURITY CLASS. *(of this report)* Unclassified
		15a. DECLASSIFICATION/DOWNGRADING SCHEDULE
16. DISTRIBUTION STATEMENT *(of this Report)* Approved for public release; distribution unlimited		
17. DISTRIBUTION STATEMENT *(of the abstract entered in Block 20, if different from Report)*		
18. SUPPLEMENTARY NOTES		
19. KEY WORDS *(Continue on reverse side if necessary and identify by block number)* Relaxation Ionization Shockwaves Vibrational relaxation Airshock Nonequilibrium chemical flow Air chemistry		

20. ABSTRACT *(Continue on reverse side if necessary and identify by block number)*

Relaxation phenomena associated with strong shock waves in air are examined in preparation for evaluation of the mechanisms which produce airshock radiant light. A model for the airshock relaxation region is described which considers air chemistry, O_2 and N_2 vibrational relaxation, and separate electron/atom energy distributions. Results from calculations are compared with experimental data for a Mach number range M = 7 - 36 with very good agreement obtained for the range M = 7 - 20.

Comparisons for post-shock equilibrium conditions, ionizational relaxation times, vibrational relaxation times for O_2 and N_2, and O_2 dissociation lengths are included.

NOLTR 74-182   1 October 1974

RELAXATION BEHIND STRONG SHOCK WAVES IN AIR

This report summarizes work performed during a two year National
Research Council Postdoctoral Research Associateship appointment
which ended 30 June 1974.

This task was initiated to provide a flow field model for the
relaxation region of an explosion shock wave in air to be used in
an investigation of airshock radiant light output; in particular,
the model was developed for use in studying the appearance of
non-luminous airshocks produced by chemical explosions observed
by Dr. L. Rudlin, the scientific advisor for this project.

The task was divided into two steps. The first step, the development
of the airshock relaxation region model, was accomplished; however,
time did not permit significant work on the second step of the task,
the formulation of the radiation model.

This study was sponsored by Work Unit number MAT-03L00010324, Task
Area number ZROO-001-010 under cognizance of the Independent
Research (IR) Panel.

                              ROBERT WILLIAMSON II
                              Captain, USN
                              Commander

                              D. C. HORNIG
                              By direction

CONTENTS

Page

ILLUSTRATIONS

Figure   TITLE

ILLUSTRATIONS (Continued)

TABLES

RELAXATION BEHIND STRONG SHOCK WAVES IN AIR

1. INTRODUCTION

Physical and chemical relaxation phenomena associated with a strong shock wave in air are discussed in this report. The investigation was performed for future evaluation of mechanisms whereby radiant light is produced in an airshock. RUDLIN (1970)* observed nonluminous airshocks produced by chemical explosions (HE) for Mach numbers on the order of 20 at sea level conditions. This absence of expected radiation corresponding to post-shock equilibrium conditions prompted this investigation.

The work discussed here is concerned with flow relaxation effects exclusive of radiation considerations. The philosophy is to provide a computational model for the flow field which may then be used to determine the radiation field separately. This technical report compares calculations for shocked equilibrium conditions, ionizational relaxation times, O_2 and N_2 vibrational relaxation times, and O_2 half-dissociation lengths with experimental data. Computations for the following flow conditions are discussed: $T = 300°K$, $P = 5$ Torr, and a Mach number range $M = 7-36$. The pressure of 5 Torr is selected so that calculations can be compared with available experimental data. The Mach number range is chosen to conform with the flow conditions investigated by RUDLIN (1970).

The airshock chemistry model and the computer code used for this study were originally developed by SHERMAN (1968)**. The present airshock relaxation model is introduced by listing the important assumptions.

(1) One-dimensional steady flow assumed.

(2) Effects of viscosity, thermal conductivity, and molecular transport neglected.

---

*References are listed in 7. REFERENCES of text in alphabetical order.
**The author wishes to acknowledge several helpful conversations with Dr. Sherman concerning his model and computer code.

(3) Effects of radiation on flow field neglected.

(4) Translational equilibrium of all chemical species assumed, exception - separate free-electron/bound-electron equilibrium allowed.

(5) Internal equilibrium assumed for rotation and vibration; exceptions - separate vibrational relaxation allowed for O_2 and N_2.

(6) Specific thermodynamic and chemical model selected.

The Sherman airshock chemistry model includes bremsstrahlung and free-bound radiative recombination of N^+ and O^+. The radiation model is not considered here.

Improvements incorporated into the airshock relaxation model include vibrational relaxation of O_2 and N_2 and separate electron/atom temperature determinations. Also, the Sherman airshock chemistry model (1968) has been updated with more recent (1972) thermodynamic and chemistry data.

LIN and TEARE (1963) present a theory for ionizational relaxation which agrees with experimental data for the Mach region M = 7-20*. BIBERMAN and YAKUBOV (1965) provide a theory for M>29 and ZHELEZNYAK and MNATSAKANYAN (1968) consider the region M = 26-36 as do ZHELEZNYAK, MNATSAKANYAN, and YAKUBOV (1971). They each cover the important transition region M = 26-29 within which the primary mechanism for determining ionizational relaxation changes from control by collisions of heavy particles to control by electron-heavy particle collisions. The present theory is applicable for the Mach number regime M = 7-36.

Results from the present calculations are compared with available experimental data. The results are summarized as follows:

1. Excellent agreement obtained for post-shock equilibrium conditions, M = 7-36.

2. Ionizational relaxation times fall well within the scatter of data for M = 7-20. However, there is only fair agreement for the range M = 26-36.

3. O_2 dissociation lengths follow available data for M = 8-16.

4. Vibrational relaxation times for O_2 and N_2 are reasonable for the range M = 7-26. However, the model is inadequate for N_2 vibrational relaxation for M > 26.

---

* The theory of LIN and TEARE (1963) is valid to M ∿ 26 with respect to ionizational relaxation since it is believed that the same ionization mechanism is dominant. However, there is no experimental data for comparison between M = 20-26.

2. THEORY

Air is assumed to contain 11 species, O_2, N_2, O, N, NO, O_2^+, N_2^+, O^+, N^+, NO^+ and e. The pre-shock species are N_2(79%) and O_2(21%). Applying conservation equations for charge neutrality and oxygen and nitrogen atoms reduces the number of independent species conservation equations from 11 to 8. The eight equations chosen may be expressed in the form*

$$\frac{d}{dx}(X_i) = \frac{-1}{2nu}(A_{ij})(K_j) \qquad i,j = 1,\ldots,8$$

where X_i represents the mole fraction of the chemical species i and K_i is the rate of production of particles of species i per unit volume. Matrix A_{ij} and the 50 reaction rates used are presented in APPFNDIX A.

The production terms are defined in the manner described by SHERMAN and KIRK (1965).

The types of chemical reactions considered are:

1. Dissociation - association

2. Rearrangement

3. Ionization - recombination

4. Positive-Ion charge exchange

The following reaction rates are evaluated at the local translational (atom) temperature: dissociation, association, rearrangement, neutral-neutral collisional ionization, and positive-ion charge exchange. The reaction rates for electron-neutral collisional ionization and electron-ion recombination are evaluated at the local electron temperature. The dissociation rates for N_2 and O_2 are corrected for vibration-dissociation coupling using factors developed by HAMMERLING, TEARE, and KIVEL (1959). See APPFNDIX A.

Vibrational relaxation is considered for species O_2 and N_2. The relaxation equation for vibrational energy for each species contains the following contributions,

---

*See 6. LIST OF SYMBOLS of text for complete definition of terms.

$$\frac{dE_v}{dx} = \text{Collisional - Vibrational energy exchange}$$

+

Dissociational - Vibrational energy exchange

+

Electron - Vibrational energy exchange (N_2 only)

Collisional-vibrational energy exchange considers the direct conversion of the energy of the colliding particles into excitation of the vibrational energy modes. The characteristic relaxation times required for computing this term for N_2 and O_2 are taken from empirical fits to experimental data provided by MILLIKAN and WHITE (1963). The second term couples the effects of the dissociation process to the vibrational relaxation rate. Vibrational energy is lost or gained for each dissociation or association event, and the number of oscillators changes during the dissociation-association process (TREANOR and MARRONE (1962)). The third term is only important for N_2 and represents energy exchange between free electrons and the molecular oscillators. This term will be discussed in connection with the electron energy equation. See APPENDIX B for the explicit formulation of this vibrational relaxation equation.

Vibrational energy exchange between N_2 and O_2 species is not considered in this model. GENERALOV, LOSEV, and OSIPOV (1964) showed that the major effects of vibrational energy transfer occur for moderate Mach numbers corresponding to final equilibrium temperatures less than 3000°K. TURCHAK (1968) considers a Mach number of M = 12 for an ambient pressure of 10^{-3} atmospheres to be an upper limit for needing to include vibrational energy exchange. However, Turchak (as do Generalov, Losev, and Osipov) neglects dissociation and ionization processes. Since the vibrational relaxation time for N_2 is of the same order of magnitude for these flow conditions as the dissociation time for O_2, the above stated conclusions represent overestimates for the effects of vibrational energy exchanges. For this reason vibrational energy exchange between N_2 and O_2 is neglected for the present calculations which extend down to M = 7.

The electron energy equation is given as

$$\frac{dT_e}{dx} = \frac{\sum_1^5 Q_i}{\frac{3}{2} n_e uk} - \frac{T_e}{n_e} \frac{dn_e}{dx}$$

4

which is a modified version of the general expression presented by
BIBERMAN AND YAKUBOV (1965). The differences include substitution of
heavy particle velocity for electron velocity and deletion of
negligible terms accounting for convection and electron thermal
conduction (BIBERMAN, MNATSAKANYAN, and YAKUBOV (1971)).

The latter investigators are able to reduce the electron energy
equation still further to the "quasistationary form" in which the
terms containing the derivatives $\frac{dT_e}{dx}$ and $\frac{dn_e}{dx}$ are neglected. What is
left is the $\sum_1^5 Q_i$ term which represents the local electron energy
balance. The quasistationary form of the equation is not appropriate
for the present calculation; the derivative terms are not negligible.

Five energy flux terms are included in the electron energy balance:

Q_1 - Energy gained by electrons through elastic collisions with
ions

Q_2 - Energy lost by electrons through electron-neutral collisional
ionization reactions

Q_3 - Energy gained by electrons through inelastic collisions with
N_2 molecular oscillators

Q_4 - Energy gained by electrons from associative ionization
reactions

Q_5 - Energy lost by electrons maintaining the quasistationary
population of excited states.

APPENDIX C provides more detailed information on the electron energy
equation.

In addition to the above set of equations, the integrated equations
for conservation of mass, momentum, and energy must be satisfied and
an equation of state is required. The conservation equations written
in a coordinate system moving with the shock front at velocity U are
written as

$$\rho u = \rho_o U$$

$$p + \rho u^2 = p_o + \rho_o U^2$$

$$h(T, TVO2, TVN2, T_e, X_i) + \frac{u^2}{2} = h(T_o, (X_i)_o) + \frac{U^2}{2}$$

Enthalpy is defined in APPENDIX D. The equation of state for a partially ionized gas mixture with a separate electron temperature is

$$p = n \, k \, (T + X_e \, (T_e - T)).$$

3.   NUMERICAL METHOD

Conventional numerical methods such as Runge-Kutta or predictor-corrector are not adequate for integrating the ordinary differential equations of one-dimensional chemical nonequillibrium flow.   The maximum allowable step size needed for such integration using these techniques is very small and extensive machine time can be required for the calculations.   The step-size requirement of the conventional methods is due to the "stiff" nature of the differential equations.   This term is defined as follows (SHERMAN (1968)); the ith equation of the system

$$\frac{dy_i}{dx} = f_i(y_1, y_2, \ldots y_n, X) \qquad i=1,\ldots,n$$

is said to be stiff in y_j if a small change in y_j causes a large change in f_i.

Several methods for handling stiff equations with discussions of step size control and stability criteria are described in SHERMAN (1968) and LOMAX and BAILEY (1967).   The technique used to solve the eight species production equations simultaneously is the two-term complete matrix method with local linearization applied which is now described briefly.

The original differential equation, shown above, is replaced by the simple approximate form* (SHERMAN (1968))

$$\frac{dy_i}{dx} = -\sum_j P_{ij} (y_j - y_{i1}) + A_i \quad i,j=1,\ldots,n$$

with the following definitions

point 1. $x = x_1$, $y_j = y_{j1}$

point 2. $x = x_1 + h$, $y_{j2} = y_{j1} + hf_{j1}$

$f_{ik} = \dfrac{dy_i}{dx}$ at $x = x_k$, $y_j = y_{jk}$, $y_m = y_{mi}$, $m{\neq}j$

$P_{ij} = -\dfrac{(f_{i2}-f_{i1})}{(y_{j2}-y_{j1})}$

---

* The approach to local equilibrium via exponential decay
 $dy/dx = -P(y-y_{eq})$ suggests the approximate form.

$$A_i = \frac{dy_i}{dx} \text{ at } x = x_1, \ y_i = y_{i1}$$

In determining P_{ij}, the jth column is determined by permitting only y_j to vary and holding all other y_m ($m \neq j$) to the initial values.

After changing to the simple approximate form, the equations are then transformed into canonical form by diagonalizing the matrix P_{ij} assuming distinct eigenvalues. The transformed system of equations is solved and then the solution in terms of the original variables is recovered using the inverse transformation. The matrix methods used to accomplish this are described in SHERMAN (1968) along with a discussion of how complex eigenvalues and identical eigenvalues are handled.

The differential equations for vibrational relaxation of O_2 and N_2 and electron energy are solved separately using the same approximate form. Matrix methods are not required since the three equations are uncoupled after they are linearized. However, the order in which the equations are solved should be noted. First, the eight species production equations are solved simultaneously, followed by the separate vibrational relaxation equations, and then the electron energy equation. After these equations are solved for the increment h, the integrated equations for conservation of mass, momentum, and energy along with the equation of state must be satisfied. This is accomplished by iteration. Newton's method is used.

A stability and truncation error analysis has not been performed for the numerical integration method used here; however, SHERMAN (1968) does prove convergence for use of the simple approximate form. The corresponding computer program is not in the production stage; all input data do not produce stable solutions and sufficient cases have not been calculated to establish more than just general guidelines for choices of initial conditions.

All calculations were performed on a CDC 6500 digital computer and the program is coded in FORTRAN IV. Computer program documentation, brief subroutine descriptions, and input data information (initial conditions) is not provided in this report but can be made available upon request to the author.

4. RESULTS

4.1 Post-Shock Equilibrium Conditions

The shocked equilibrium conditions attained following relaxation using the airshock relaxation code have been compared with calculations from WILLETT and LEHTO (1958) for a Mach number range M = 7-36 with ambient conditions: T = 300°K, p = 5 Torr. The results of WILLETT and LEHTO (1958) are obtained by solving the normal shock (Rankine-Hugoniot) relations without considering relaxation mechanisms. The corresponding properties of the final equilibrium state agree within 1% for the variables of temperature, density, pressure, and velocity. Electron number density results obtained with the airshock relaxation code agree on the order of 15% with equilibrium properties tabulated by HILSENRATH and KLEIN (1965). Although the detailed results are not presented here, the comparisons do indicate that proper post-shock equilibrium conditions are calculated with the airshock relaxation code.

4.2 Relaxation Region Solution

Figures 1-4 display the relaxation region solution obtained for the flow conditions: M = 16.47, p = 5 Torr, T = 300°K, which are in the regime studied by LIN and TEARE (1963) and SCHÄFER and FROHN (1972). LIN and TEARE (1963) employ "one-way coupling" between the processes of dissociation and ionization which is satisfactory when the degree of ionization is less than ∿1%; the temperature, density, and chemical composition profiles are determined (including O_2 and N_2 vibrational relaxation) without considering ionization processes. The ionization solution is then completed using the determined flow field. SCHÄFER and FROHN (1972) solve the coupled chemical and ionizational relaxation equations without considering vibrational relaxation.

A comparison between Figure 1 and Figure 3 indicates that NO^+ is the predominant ion. Figure 2 displays the early disappearance of O_2 and the appearance of an NO peak. These are expected results for these flow conditions (LIN and TEARE (1963)). The temperature profiles presented in Figure 4 show strong coupling between N_2 vibrational energy and the electron energy. This is in agreement with the free-electron/N_2-vibrational model and results discussed by ZHELEZNYAK and MNATSAKANYAN (1968). Initially, for the present calculations, the free electrons are assumed to be in equilibrium with the N_2 vibrators. At the point where the particle time increment between calculation steps becomes an order of magnitude larger than the time required for free electrons to establish a Maxwell-Boltzmann distribution, separate N_2-vibrator and free-electron/bound-electron energy relaxation is permitted. This transition is indicated in Figure 4 by the appearance of a dip in the electron temperature. After several steps

9

(10 for this calculation), the electrons approach equilibrium with the N_2-vibrators.

The O_2 vibrational temperature profile in Figure 4 exhibits a pronounced peak whereas the N_2 vibrational temperature does not for these flow conditions. This behavior is described in the paper by TREANOR and MARRONE (1962) from which the model for vibrational relaxation (with no N_2-vibrational/free-electron coupling) used in these calculations is taken.

Figures 5 and 6 correspond to the relaxation region solution for the conditions: M = 26.76, p = 5 Torr, T = 300°K. The electron number density profile in Figure 5 is quite different from the profile in Figure 1 (M = 16.47). Figure 6 indicates that N_2^+ and O^+ are the predominant ions. The associative ionization reactions, $N+O \rightleftharpoons NO^+ + e$ is the main ionization mechanism up to M∿26; however, for M>26 reactions such as $N+N \rightleftharpoons N_2^+ + e$ and $O+e \rightleftharpoons O^+ + 2e$ predominate. The general trend is that the main ionization mechanism shifts from associative ionization to electron-neutral collisional ionization for increasing Mach numbers beyond M∿26.

BIBERMAN and YAKUBOV (1965) and ZHELEZNYAK and MNATSAKANYAN (1968) provide additional discussion on ionization mechanisms for M>26.* The former present an ionizational relaxation model appropriate for M>29; the lower limit due to the restrictive assumption that the dissociation process for O_2 and N_2 are considered complete before the onset of ionization. ZHELEZNYAK and MNATSAKANYAN (1968) provide an ionizational relaxation model satisfactory for M>26. In this case the dissociation of N_2 is solved simultaneously with ionization and O_2 is assumed completely dissociated, initially.

4.3 Ionizational Relaxation

Figure 7 provides a comparison between available experimental data and the present calculations for ionizational relaxation time as a function of Mach number for the range M = 7-36. Other solutions for portions of this Mach number range which have been discussed briefly in section 4.2 Relaxation Region Solution of text are presented in BIBERMAN, MNATSAKANYAN, and YAKUBOV (1971). Experimental data from eight sources are included in Figure 7.** Ambient pressures for these experiments range from 0.05 to 10 Torr. Since the ionization mechanism is a binary collision process, ionizational relaxation times are pressure-scaled for purposes of data reduction. Pressure scaling has been verified for these calculations which do not include effects of radiation.

---

*ZHELEZNYAK (1973) discusses ionization relaxation in nitrogen for M = 50-73.
**Experimental data plotted in Figure 7 are taken from graphs provided by the cited references.

The Mach number range presented in Figure 7 can be separated into three subregions established by the distribution of experimental data. The first subregion, M = 7-20, is well defined by data of SCHAFER and FROHN (1972) and LIN, NEAL, and FYFE (1962). Other data found in the literature are included in the figure.* For this region the definition of ionizational relaxation time (laboratory coordinates) for the theoretical model is taken to be the time for the electron number density to attain 90% of the peak value. The calculated curve compares best with the data of SCHÄFER and FROHN (1972) for the range M = 7-20.

No data have been located in the range M = 20-26 for comparisons with calculations. Two additional definitions for ioniza- tional relaxation time are employed for the computations which give equivalent results for this region with agreement on the order of 10%. The definition used in Figure 7 is as follows: The time (laboratory coordinates) between the shock front and the time at which a line drawn through the maximum slope of the electron number density profile reaches the equilibrium value. Another definition which is also checked is one used by WILSON (1966) for analysis of experimental results in the range M = 26-36. An infrared radiation model which includes bremsstrahlung and recombination continuum for oxygen and nitrogen (from Wilson (1966)) is used to calculate a radiation profile for the relaxation region at a wavelength of 6.1μ. The relaxation time is then defined to be the time (laboratory coordinates) between the shock front and the time at which a line drawn through the maximum slope of the infrared radiation profile reaches the equilibrium value.

The range M = 20-26 contains a portion of the transition region for the shift in the ionizational relaxation mechanisms dis- cussed in section 4.2 Relaxation Region Solution of text. The cal- culations evidence this shift in Figure 7. The lack of data in this region does leave to question the proper location for the shift in ionization mechanisms.

The comparison between the present calculations and the experimental results of WILSON (1966) for the range M = 26-36 indi- cates only fair qualitative agreement. The definition of ionizational relaxation time for this region is the same as that for M = 20-26 and is equivalent to the definition used by WILSON (1966). Because of the transition in ionization mechanisims there is a peak in the relaxation times as a function of Mach number. The theoretical and experimental locations for this peak do not agree. Modifications have not been made to the model which account for this disagreement. No radiation model has been included for iteration with the flow field model for strong radiative-gasdynamic coupling effects described by CARLSON (1972) for M>29. It should be pointed out, however, that ZHELEZNYAK and MNATSAKANYAN (1968) obtain good agreement with the data of

---

*LIN, NEAL, and FYFE (1962) discuss the discrepancies between their data and the earlier results of NIBLETT and BLACKMAN (1958) and the data of MANHEIMER-TIMNAT and LOW (1959).

WILSON (1966) for these flow conditions without including effects of radiative-gasdynamic coupling. Also, no adjustments of selected reaction rates nor addition of kinetic equations for individual excited states of atomic nitrogen and oxygen (as considered by ZHELEZNYAK and MNATSAKANYAN (1968)) have been included to obtain better agreement between the results of the present formulation and the data of WILSON (1966).

4.4 O_2 Dissociation

The variation of O_2 half-dissociation length with Mach number for the range M = 8-22 is given in Figure 8. The solid curve shown in the figure is derived from results obtained with the airshock relaxation computer code. For these calculations the O_2 half-dissociation length is defined as the location in the relaxation region where the mole fraction of O_2 attains the value $X_{O_2} = ((X_{O_2})_{INITIAL} + (X_{O_2})_{FINAL})/2$.

Experimental results from STRICKER and LOW (1972) and LIN and FYFE (1961) are included for comparison. Pressure scaling is used to convert the experimental data to the proper ambient conditions. The calculations are on the high side but are within a factor of two for the low Mach number region M = 8-10 and the calculations are within the scatter of data for the high Mach number region, M = 14-21. The calculations for the latter range, however, do tend to fall off more rapidly than the data indicate. STRICKER and LOW (1972) present additional theoretical curves for O_2 half-dissociation length dependence on Mach number which do not agree as well with the experimental results for the entire range as do the present calculations.

4.5 Vibrational Relaxation

Results for vibrational relaxation of O_2 and N_2 using the airshock relaxation computer code are given in Figure 9. Vibrational relaxation in particle coordinates, not laboratory coordinates as used in Figures 1-7, is plotted versus temperature.

The expression for vibrational relaxation is defined in APPENDIX B. The main contribution to vibrational relaxation and in many cases the only contribution considered, is collisional-vibrational energy exchange. This contribution pressure scales due to collisional dependence thus justifying the use of $p\tau$ ordinates in Figure 9. The Landau-Teller theory (MILLIKAN and WHITE (1963)) postulates inverse cube root temperature dependence for vibrational relaxation which is the reason behind the choice of the temperature function for the abscissa of Figure 9. Also included in the figure are empirical fits to experimental data for vibrational relaxation of O_2 and N_2 established by MILLIKAN and WHITE (1963) using the Landau-Teller theory as a guide for functional dependence of important parameters involved with the interaction. The MILLIKAN and WHITE (1963) model only considers collisional-vibrational energy exchange. This same model is used for the collisional-vibrational energy exchange contribution in the present calculation. For N_2, additional contributions to

vibrational relaxation from the dissociation/association process for N_2 and free-electron/N_2-vibrator energy exchange are included. For O_2, the additional contribution from the dissociation/association process for O_2 is included. The difference between the MILLIKAN and WHITE (1963) results and the present results in Figure 9 is attributable in most part to the additional contributions discussed above for the present model. Another reason for differences between the two results follows from the definitions of pressure and temperature used to convert the present calculations to $p\tau$-$T^{-\frac{1}{3}}$ coordinates*. The local temperature and pressure values used for the airshock relaxation results correspond to the flow conditions just downstream of the translational/rotational shock; that is, the initial temperature and pressure in the relaxation region before chemical, vibrational, electronic, and ionizational relaxation processes have begun. However, if the airshock relaxation results in Figure 9 were corrected to correspond to the local pressure and temperature at the location of the peak vibrational temperature, which would represent the end of the vibrational relaxation region, then the results would be modified at most on the order of 10%; approximately 7% change for temperature and 3% change for pressure. It is for this reason that the results are plotted using $p\tau$-$T^{-\frac{1}{3}}$ coordinates along with the MILLIKAN and WHITE (1963) results even though contributions from relaxation processes other than direct collisional-vibrational energy exchange are included.

The net effect of including the contributions of the dissociation/association processes, and in the case of N_2 also including free-electron/N_2-vibrator coupling, in the vibrational relaxation model is to reduce the relaxation time as evidenced in Figure 9. The higher the Mach number, or temperature, the greater the reduction in relaxation time for both N_2 and O_2.

For the higher Mach numbers, $M>26$ or ($T^{-1/3}$) values less than 0.030 in Figure 9, the vibrational relaxation model used is not satisfactory. The $p\tau$ range is of the order of collision times and assumptions for the vibrational relaxation model such as the establishment of Maxwell-Boltzmann distributions are just not satisfied. However, in this Mach number range, $M>26$, vibrational contributions to other relaxation processes such as ionization become less important. The calculations indicate that the dissociation of O_2 can be considered complete before the onset of ionization for $M>26$ (ZHELEZNYAK and MNATSAKANYAN (1968)) and N_2 can be considered completely dissociated before ionization begins for $M>29$ (BIBERMAN and YAKUBOV (1965)). Therefore, only improvement of the vibrational relaxation model for N_2 through the range $M = 26-29$ is needed.

---

* $p\tau$ versus $T^{-\frac{1}{3}}$

4.6 Electron Energy Relaxation

An example of an electron temperature profile for the relaxation region is provided in Figure 4. The discussion presented in section 4.2 Relaxation Region Solution of text will not be repeated here except to again point out the strong energy coupling between the N_2 vibrators and the free electrons indicated in the figure. The electron energy equation which is used to calculate this profile is defined in APPENDIX C.

For the lower Mach number range M = 7-12* calculations indicate that the electron energy approaches final shocked equilibrium conditions very rapidly, on the order of the time it takes to establish a separate electron Maxwell-Boltzmann distribution. The electron temperature then remains essentially constant throughout the rest of the relaxation region. Therefore, calculation time can be reduced by assuming that the electron temperature equals the post-shock equilibrium temperature throughout the relaxation region for the above stated flow conditions.

Within the range M = 12-20 the main contribution to the calculation by including a separate electron temperature is in reducing the amount of energy transferred to the N_2 vibrators over most of the relaxation region. When T_e is constrained to follow the atom translational temperature, then the N_2 vibrators appear to be in near equilibrium with translation for most of the relaxation region. However, if a separate electron temperature is permitted, then the free electrons and the N_2 vibrators are in near equilibrium for a major portion of the relaxation region and they together approach equilibrium with translation much more slowly.**

Above M∿20 the main contribution for including a separate electron temperature shifts from modifying the N_2-vibrator energy distribution to proper evaluation of reaction rates for electron-atom collisional ionization and electron-ion recombination. These reaction rates depend on the free electron energy distribution (temperature) and an evaluation of the reaction rates at the higher atom translational temperature is in error.

For M>25 considerable calculation time is consumed by considering a separate electron temperature. This calculation time can be greatly reduced by setting the electron temperature equal to the N_2 vibrational temperature at all points in the relaxation region. This is a reasonable assumption because of the strong energy coupling between the free electrons and the N_2 vibrators; there is near equilibrium between them over most of the relaxation region.

*Mach number ranges quoted in this section are only approximate. A sufficient number of cases have not been investigated to make truly accurate determinations.
**The free-electron/N_2-vibrator coupling terms are not considered when the free electron temperature is constrained to follow the translational temperature.

14

5. SUMMARY AND RECOMMENDATIONS

A model for the relaxation region behind shock waves in air has been developed. It is not the first such model. However, other models to date are only satisfactory for portions of the Mach number range, M = 7-36, considered here. Within this range the ionizational mechanism shifts from associative ionization to electron-neutral collisional ionization and many air chemical reactions change in relative importance with respect to one another.

This model has been developed for use in determining radiation output from airshocks. The airshock relaxation region is determined so that the flow properties may be used to calculate the radiation properties for the region. One-way coupling is employed. The flow field determines the radiation field but it is assumed that the radiation field does not affect the flow field appreciably. The present calculations may be considered the first step in an iteration process in which the computations are terminated when the flow field and radiation field results for consecutive cycles agree within stated limits. The radiation calculations have not been performed using this model.

The summary of results to follow in subsequent paragraphs is separated into five Mach number ranges which have been determined by:

1. The distribution of experimental data.

2. The shift of the predominant ionization mechanism from associative ionization to electron-neutral collisional ionization.

3. The change in character of the separate electron/atom energy distributions.

In addition to comments concerning agreement between calculated and experimental results for each Mach number range, important considerations such as the predominant ionization mechanism, the status of O_2 and N_2 dissociation and vibrational relaxation, and the properties of the separate electron/atom energy distributions are noted. Refer to Figures 7, 8, and 9 for comparisons concerned with ionizational relaxation times, O_2 dissociation distances, and vibrational relaxation times for O_2 and N_2 respectively.

M = 7-12   Associative ionization is the predominant ionization
              mechanism.
           O_2 and N_2 dissociation and vibrational relaxation must be
              considered.
           Electron temperature is essentially equal to the post-shock
              equilibrium temperature throughout the relaxation region.

Calculations for post-shock equilibrium conditions agree
with standard Rankine-Hugoniot results.
Calculations for ionizational relaxation times are within
scatter of data.
Calculations for O_2 dissociation distances are within scatter
of data.
Reasonable values for O_2 and N_2 vibrational relaxation times
are calculated with model.

M = 12-20 Associative ionization is the predominant ionization
mechanism.
O_2 and N_2 dissociation and vibrational relaxation must be
considered.
Separate electron and N_2-vibrator energy distributions are
in near equilibrium for most of the relaxation region.

Calculations for post-shock equilibrium conditions agree
with standard Rankine-Hugoniot results.
Calculations for ionizational relaxation times are within
scatter of data.
Calculations for O_2 dissociation distances are within scatter
of data. No data available above M = 16.
Reasonable values for O_2 and N_2 vibrational relaxation times
are calculated with model.

M = 20-26 Associative ionization is the predominant ionization
mechanism.
O_2 and N_2 dissociation and vibrational relaxation must be
considered.
Separate electron and N_2-vibrator energy distributions
are in near equilibrium throughout most of the relaxation
region.

Calculations for post-shock equilibrium conditions agree
with standard Rankine-Hugoniot results.
No experimental data for ionizational relaxation times are
available. Theoretical model indicates abrupt changes
in Mach number dependance of ionizational relaxation times
within range M = 25-26.
Reasonable values for O_2 and N_2 vibrational relaxation times
are calculated with model.

M = 26-29 The predominant ionization mechanism shifts from associative
ionization to electron-neutral collisional ionization.
N_2 dissociation and vibrational relaxation must be
considered.
Electron temperature is essentially equal to local N_2
vibrational temperature throughout most of the relaxation
region.

Calculations for post-shock equilibrium conditions agree
with standard Rankine-Hugoniot results.

Calculations for ionizational relaxation times follow
qualitatively the abrupt change in Mach number dependence
of data. However, the calculations do fall below the data
and the pronounced peak indicated in the data (Figure 7)
is not followed by the calculations.

The vibrational relaxation model is not adequate for the
range. Unrealistically short relaxation times are
calculated for N_2 vibrators.

M = 29-36 Electron-neutral collisional ionization is the predominant
ionization mechanism.

N_2 vibrational relaxation must be considered.

Electron temperature is essentially equal to local N_2
vibrational temperature throughout most of the relaxation
region.

Calculations for post-shock equilibrium conditions agree
with standard Rankine-Hugoniot results.

Calculations for ionizational relaxation times do not follow
Mach number dependence of data.

The vibrational relaxation model is not adequate for this
range. Unrealistically short relaxation times are
calculated for N_2 vibrators.

The following modifications to the airshock relaxation model are
recommended so as to obtain better agreement between calculations
and experimental data for the Mach range M = 26-36.

1. The existing set of chemical reaction rates should be adjusted
on an individual reaction basis in order to optimize agreement between
calculations and data.

2. Reactions which account for individual excited state
populations of atomic nitrogen and oxygen should be added to the set
of reactions.*

The above two modifications to the model should then be followed
by iterations between flow field calculations (the type of calculations
presented in this report) and radiation output calculations (to be
developed). The actual effects of radiation of the flow field can
then be determined.

Also, the vibrational relaxation model needs to be modified for
the same Mach number range, M = 26-36. The present model defines
vibrational temperatures in the relaxation region at unrealistically
early times. This procedure can be corrected by not defining a

---

*ZHELEZNYAK and MNATSAKANYAN (1968) obtained good agreement with
experimental data for ionizational relaxation times within this
Mach number range by having included these reactions and by not
having included radiative-gasdynamic coupling.

vibrational temperature before a sufficient number of collisions have
occurred to establish a Maxwell-Boltzmann distribution of vibrators.
This modification will also affect the early-time definition of the
electron temperature. The vibrational temperatures (N_2) and the
electron temperature can be evaluated at the pre-shock (ambient)
conditions throughout this initial relaxation region.

NOTE ADDED IN PROOF

Two recent papers concerned with results of interest to the
present investigation came to the attention of the author
prior to publication of this report.

Chan and Glass* present experimental data which fall within
the data boundaries of WILSON (1966) and follow closely the
ionizational relaxation theory of ZHELEZNYAK and MNATSAKANYAN
(1968) for the Mach range M = 28-35. These results provide
an additional indication that the airshock relaxation model,
the subject of this report, should be modified as discussed
in section 5. SUMMARY AND RECOMMENDATIONS of the text to
obtain better agreement with data in this flow regime.

Lazdinis and Petrie** report on recent theoretical and
experimental results concerned with free electron and
N_2-vibration energy coupling for weakly ionized nozzle
expansions of shock-heated nitrogen. Although the nozzle
expansion flow conditions are quite different from airshock
relaxation flow conditions, the formulations for the electron
energy equations are similar; differences arise due to the
relative importance of the individual electron energy flux
terms. The main coupling mechanism for both flows is the
same; that is free-electron/N_2-vibrator energy exchange.

*Chan, S. K. and Glass, I. I., "Radiative Relaxation Behind High-Speed
 Shock Waves in Air," Physics of Fluids 17, No. 4, 1974
**Lazdinis, S. S. and Petrie, S. L., "Free Electron and Vibrational
 Temperature Nonequilibrium in High Temperature Nitrogen", Physics
 of Fluids 17, No. 8, 1974

6.   LIST OF SYMBOLS

A
- Constant used in definition of chemical reaction rate, units are $(CM^3)^j/SEC$ for which $j = 0,1$, or 2 depends on the reaction being of first, second, or third order.

A_i
- Coefficient of constant term in the approximate form for f_i.

A_{ij}
- Coefficient matrix used for system of species conservation equations.

a_e
- Average electronic excitation cross section for free-electron impact, CM^2.

B
- Constant used in definition of chemical reaction rate for temperature power dependence.

C
- Constant used in definition of chemical reaction rate which represents activation energy in temperature units, °K.

$(D_{ea})_i$
- Net production rate, forward minus reverse, for the ith electron-neutral collisional ionization reaction CM^3/SEC.

E_i
- Electron excitation energy for chemical species i, ERGS.

E_v
- Vibrational energy, ERGS.

$(E_v)_{VIB. EQ.}$
- Vibrational energy evaluated at local translational/vibrational equilibrium conditions, ERGS.

E_{I_i}
- Ionization energy of chemical species i, ERGS.

$e(t)$
- Partition function for N_2 harmonic oscillator.

f_i
- Derivative of species y_i with respect to x.

f_{ij}
- Derivative of species y_i with respect to x evaluated at the jth point.

g_i
- Statistical weight of ith electronic energy level.

h
- Step size for numerical integration, CM.

h(T)   - Enthalpy, ERGS/GM

h_F - Enthalpy of formation, ERGS/GM-MOLE.

K   - Chemical equilibrium constant

K_i - Rate of production of species i per unit volume, CM^{-3}/SEC.

k   - Boltzmann constant, ERG/°K.

k_d - Dissociation reaction rate corrected for vibrational relaxation effects, CM^3/SEC.

$(k_d)_{VIB.\ EQ.}$ - Dissociation reaction rate evaluated for translational/vibrational equilibrium, CM^3/SEC.

k_f, k_r - Forward and reverse chemical reaction rates, units are defined for SYMBOL A.

$(k_{AI})_f$, $(k_{AI})_r$ - Forward and reverse associative ionization reaction rates, CM^3/SEC.

k_{RR} - Chemical reaction rate, units are defined for SYMBOL A.

M   - Mach number.

m_i - Mass of ion species i, GM.

N   - Number of discrete energy levels below dissociation energy for cut-off harmonic oscillator models of O_2 and N_2.

n   - Total particle number density, CM^{-3}.

n_e - Electron number density, CM^{-3}.

P_{ij} - Coefficient matrix in f_i approximate form evaluated for f_i and y_j.

P_e - Average rate constant for electronic excitation by free-electron impact, CM^3/SEC.

p   - Static pressure, DYNE/CM^2 (also Torr).

Q_i - Electron energy flux terms defined in Appendix C, i=1,5; GM/SEC^3-CM.

R   - Mass gas constant, ERG/°K-GM.

T   - Temperature, translational temperature, °K.

T_e — Electron temperature, °K.

T_m — $(T_v^{-1} + T^{-1})^{-1}$ °K.

T_v,TVN2,TVO2 — Vibrational temperature, N_2 and O_2, °K.

U — Velocity of shock front into undisturbed gas, CM/SEC.

u — Gas velocity behind shock wave in the coordinate system fixed to wave front, CM/SEC.

v_e — Electron mean velocity, CM/SEC.

X_i — Mole fraction of species i.

x — Distance coordinate, independent variable, CM.

y — Dependent variable, function of x.

y_i — Dependent variable for species i, function of x.

y_{ij} — Dependent variable for species i evaluated at point j, function of x.

y_{eq} — Dependent variable evaluated at local equilibrium conditions, function of x.

Z1, Z2 — Uncertainty parameters used in chemical reaction rate definition.

θ_v — Characteristic vibrational temperature, °K.

θ_i — Characteristic electronic temperature for energy level i, °K.

ρ — Gas density, GM/CM^3.

τ — Relaxation time, μSEC.

τ_L — Relaxation time, laboratory coordinates, μSEC.

τ_p — Relaxation time, particle coordinates, μSEC.

SUBSCRIPTS

i,j,k,ℓ,m — Dummy subscripts.

o — Free stream conditions, p_o, ρ_o, T_o, $(X_i)_o$.

v — Denotes vibrational relaxation quantity.

7. REFERENCES

BASHENOVA, T. V. and LOBASTOV, YU.S., "On the Mechanism of Thermal Ionization of Air," Foreign Technology Division, Air Force Systems Command, Wright-Patterson Air Force Base, Ohio, Translation FTD-MT-24-1393-71, January 1972

BIBERMAN, L. M. and YAKUBOV, I. T., "The State of a Gas behind a Strong Shock-Wave Front," High Temperature $\underline{3}$, No. 3, 309-320, 1965

BIBERMAN, L. M., MNATSAKANYAN, A. KH., and YAKUBOV, I. T., "Ionization Relaxation behind Strong Shock Waves in Gases," Soviet Physics Uspekhi $\underline{13}$, No. 6, 728-744, 1971

BORTNER, M. H., "Chemical Kinetics in a Reentry Flow Field," General Electric Co. Space Sciences Lab., King of Prussia, Pennsylvania, TIS Report R63SD63, August 1963

BORTNER M. H., "A Review of Rate Contants of Selected Reactions of Interest in Re-Entry Flow Fields in the Atmosphere," NBS Technical Note 484, May 1969

BORTNER, M. H. and BAURER, T., "Defense Nuclear Agency Reaction Rate Handbook," Second Edition Revision No. 1, DNA1948H (Formally DASA 1948), Published by DASIAC DOD Nuclear Information and Analysis Center, General Electric, TEMPO, Santa Barbara, California, November 1972

CARLSON, L. A., "Radiative Cooling and Nonequilibrium Chemistry Coupling behind Normal Shock Waves," AIAA Journal $\underline{10}$, No. 2, 230-232, 1972

FROHN, A. and deBOER, P.C.T., Physics of Fluids, Suppl. I $\underline{12}$, I-54, 1969

GENERALOV, N. A., LOSEV, S. A., and OSIPOV, A. I., "Relaxation of the Vibrational Energy of Air Molecules behind the Direct Shock Wave Front," Goddard Space Flight Center, NASA Technical Translation NASA TT F-8933, July 1964

HAMMERLING, P., TEARE, J. D., and KIVEL, B., "Theory of Radiation from Luminous Shock Waves in Nitrogen," Physics of Fluids $\underline{2}$, No. 4, 422-426, 1959

HILSENRATH, J. and KLEIN, M., "Tables of Thermodynamic Properties of Air in Chemical Equilibrium including Second Virial Corrections from 1,500 °K to 15,000 °K," Arnold Engineering Development Center, Air Force Systems Command, Arnold Air Force Station, Tennessee, AEDC-TR-65-58, March 1965

LIN, S. -C. and FYFE, W. I., "Low-Density Shock Tube for Chemical Kinetics Studies," Physics of Fluids 4, No. 2, 238-249, 1961

LIN, S. -C., NEAL, R. A., and FYFE, W. I., "Rate of Ionization behind Shock Waves in Air. I. Experimental Results," Physics of Fluids 5, No. 12, 1633-1648, 1962

LIN, S. -C. and TEARE, J. D., "Rate of Ionization behind Shock Waves in Air. II. Theoretical Interpretations," Physics of Fluids 6, No. 3, 355-375, 1963

LOMAX, H. and BAILEY, H. E., "A Critical Analysis of Various Numerical Integration Methods for Computing the Flow of a Gas in Chemical Nonequilibrium," Ames Research Center, NASA-TN D-4109, August 1967

MANHEIMER-TIMNAT, Y. and LOW, W., "Electron Density and Ionization Rate in Thermally Ionized Gases Produced by Medium Strength Shock Waves," Journal of Fluid Mechanics 6, 449-461, 1959

MILLIKAN, R. C. and WHITE, D. R., "Systematics of Vibrational Relaxation," Journal of Chemical Physics 39, No 12, 3209-3213, 1963

NIBLETT, B. and BLACKMAN, V. H. "An Approximate Measurement of the Ionization Time behind Shock Waves in Air," Journal of Fluid Mechanics 4 , 191-194, 1958

RUDLIN, L., "On the Origin of Shockwaves from Condensed Explosions in Air, Part 3: Airshock Radiation from Small Explosions at Sea-Level Conditions," Naval Ordnance Laboratory Report NOLTR 69-74, June 1970

SCHÄFER, J. H. and FROHN, A., "Ionization behind Shock Waves in Nitrogen-Oxygen Mixtures," AIAA Journal 10 No. 8, 985-987, 1972

SHERMAN, M. P. and KIRK, V. L., "New Methods of Integrating Stiff Differential Equations for Chemical Nonequilibrium Flow," General Electric Co., Space Sciences Lab., King of Prussia, Pennsylvania, TIS Report R65SD52, October 1965

SHERMAN, M. P., "Radiation Coupled Chemical Nonequilibrium Normal Shock Waves," J. Quant. Spectrosc. Radiat. Transfer 8, 569-600, 1968

STRICKER, J. and LOW, W., "Atomic Oxygen Formation Times Obtained from Measurements of Electron Density Profiles behind Shock Waves in Air," Physics of Fluids 15, No. 12, 1972

TREANOR, C. E. and MARRONE, P. V., "Effect of Dissociation on the Rate of Vibrational Relaxation," Physics of Fluids 5, No. 9, 1022-1026, 1962

TURCHAK, L. I, "Exchange of Vibrational Energy between Components of Air behind the Front of a Normal Shock Wave," Naval Intelligence Command Translation No. 2729, November 1968

WILLETT, S. E. and LEHTO, D. L., "Normal Shock (Rankine-Hugoniot) Relations for Various Altitudes from Sea Level to 300,000 Feet," Naval Ordnance Laboratory, NAVORD REPORT 6075, April 1958

WILSON, J., "Ionization Rate of Air behind High-Speed Shock Waves," Physics of Fluids 9, No. 10, 1966

ZEL'DOVICH, YA. B. and RAIZER, YU. P., "Physics of Shock Waves and High-Temperature Hydrodynamic Phenomena, Volume 1," Edited by HAYES, W. D. and PROBSTEIN, R. F. Academic Press, New York and London, 1966

ZHELEZNYAK, M. B. and MNATSAKANYAN, A. KH., "Ionizational Relaxation behind Shock Waves in Air," High Temperature 6, No. 3, 377-380, 1968

ZHELEZNYAK, M. B., MNATSAKANYAN, A. KH. and YAKUBOV, I. T., "Relaxation and Nonequilibrium Radiation behind Shock Waves in Air," NASA Technical Translation NASA TT F-13528, April 1971

ZHELEZNYAK, M. B., "Ionization Relaxation behind Shock Waves in Nitrogen at Speeds of 17 to 25 KM/SEC," Journal of Applied Mechanics and Technical Physics 11, No. 6, 1007-1011, 1973

APPENDIX A: CHEMICAL REACTION RATES

The chemical reaction rates used in the airshock chemistry model are listed at the end of this appendix in Table A-1. Types of reactions include dissociation, rearrangement, ionization, and positive-ion charge exchange with their respective inverse reactions. The reaction rates are taken from three sources: reference A1 - BORTNER (1963), reference A2 - BORTNER (1969), and reference A3 - BORTNER and BAURER (1972). The rates are listed in either the forward (k_f) or reverse (k_r) direction and are presented in the form*

$$k_{RR} = (A \pm Z1) \, (T/300)^{B \pm Z2} \, \exp(-C/T),$$

with units $(CM^3)^j \, SEC^{-1}$ for which $j = 0, 1,$ or 2 depends on the reaction being of first, second, or third order, respectively. Z1 and Z2 represent the uncertainty estimates. Better agreement between the present calculations and cited experimental results for ionizational relaxation times is obtained using the rate parameters $A' = A - Z1$ and $B' = B - Z2$.

The equilibrium constant is used to relate the rates of the opposing directions by

$$K = \frac{k_f}{k_r} \; .$$

Actually this relation only holds for reactions in which the same states (electronic, vibrational, and rotational) are attained for products and reactants. Considering the available data and the corresponding uncertainty limits, the use of the above relation is reasonable. However, for the dissociation reactions of O_2 and N_2 the vibration-dissociation coupling factor proposed by HAMMERLING, TEARE and KIVEL (1959) is used to correct the reaction rates for the dissociation process.

$$k_d = (k_d)_{VIB.EQ.} \frac{(1-e^{-N\Theta_v/T_m})}{N(e^{\Theta_v/T_m}-1)} \frac{(e^{\Theta_v/T_v}-1)}{(e^{\Theta_v/T}-1)}$$

The dissociation reaction rates are modified to account for the distribution of the vibrational states being characteristic of the local vibrational temperature and not the local translational

_____

*See 6. LIST OF SYMBOLS of text.

temperature. The assumption that $T_v = T$ when actually $T_v \neq T$ incorrectly prescribes the distribution of the vibrationally, excited states. This affects the dissociation reaction rate since the highly excited vibrational states are more easily dissociated.

The ionization reaction rate dependence on electron temperature is outlined in 2. THEORY of text.

Fifty reactions are considered, though only eight independent equilibrium constants are required. The eight reactions selected are

$$O_2 \rightleftharpoons O + O$$

$$N_2 \rightleftharpoons N + N$$

$$NO \rightleftharpoons N + O$$

$$N \rightleftharpoons N^+ + e$$

$$O \rightleftharpoons O^+ + e$$

$$NO \rightleftharpoons NO^+ + e$$

$$O_2 \rightleftharpoons O_2^+ + e$$

$$N_2 \rightleftharpoons N_2^+ + e$$
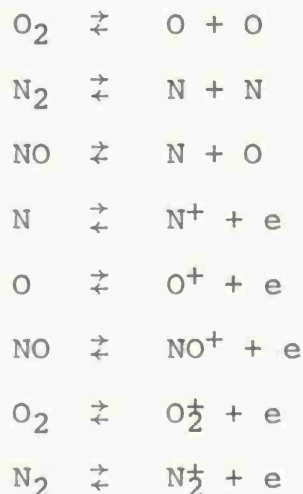
and the corresponding species conservation equations may be expressed in the form (SHERMAN (1968))

$$\frac{d}{dx}
\begin{vmatrix}
x_O \\
x_N \\
x_{NO} \\
x_{O^+} \\
x_{N^+} \\
x_{NO^+} \\
x_{O_2^+} \\
x_{N_2^+}
\end{vmatrix}
= \frac{-1}{2nu}
\begin{vmatrix}
(x_O - 2) & x_O & \alpha & 3x_O & 3x_O & 2x_O & 2x_O & 2x_O \\
x_N & (x_N - 2) & 0 & 3x_N & 3x_N & 2x_N & 2x_N & 2x_N \\
x_{NO} & x_{NO} & -2 & 3x_{NO} & 3x_{NO} & 2x_{NO} & 2x_{NO} & 2x_{NO} \\
x_{O^+} & x_{O^+} & 0 & (3x_{O^+} - 2) & 3x_{O^+} & 2x_{O^+} & 2x_{O^+} & 2x_{O^+} \\
x_{N^+} & x_{N^+} & 0 & 3x_{N^+} & (3x_{N^+} - 2) & 2x_{N^+} & 2x_{N^+} & 2x_{N^+} \\
x_{NO^+} & x_{NO^+} & 0 & 3x_{NO^+} & 3x_{NO^+} & (2x_{NO^+} - 2) & 2x_{NO^+} & 2x_{NO^+} \\
x_{O_2^+} & x_{O_2^+} & \alpha & 3x_{O_2^+} & 3x_{O_2^+} & 2x_{O_2^+} & (2x_{O_2^+} - 2) & 2x_{O_2^+} \\
x_{N_2^+} & x_{N_2^+} & 0 & 3x_{N_2^+} & 3x_{N_2^+} & 2x_{N_2^+} & 2x_{N_2^+} & (2x_{N_2^+} - 2)
\end{vmatrix}
\cdot
\begin{vmatrix}
K_O \\
K_N \\
K_{NO} \\
K_{O^+} \\
K_{N^+} \\
K_{NO^+} \\
K_{O_2^+} \\
K_{N_2^+}
\end{vmatrix}$$

The temperature dependence for the equilibrium constants corresponding to these reactions are presented in BORTNER and BAURER (1972).

Some brief comments concerning the selection of reaction rates are in order. The reaction rates presented in BORTNER (1969) represent empirical fits made to accommodate both low $(T<500°K)$ and high $(T>2500°K)$ temperature data when possible. BORTNER (1969) and BORTNER (1963) reaction rate data were compiled for reentry flow fields and are appropriate for airshock chemistry calculations. The corresponding reaction rates presented by BORTNER and BAURER (1972) are concerned with low temperature data. BORTNER and BAURER (1972); however, provide a more inclusive list and present the most recent estimates. In many cases the reaction rates compiled in BORTNER and BAURER (1972) represent estimates determined by a committee of workers knowledgeable in the field.

All positive-ion charge exchange reaction studies were performed at low temperatures. BORTNER (1969) suggests an uncertainty factor of $(T/300)^{\pm 1.5}$ for which the exponent value 1.5 is an estimate. Reaction rates for positive-ion charge exchange reactions are selected from BORTNER and BAURER (1972) for the present calculations and the temperature factor $(T/300)^{-1.5}$ is used unless otherwise specified by the references. For dissociation, rearrangement, and ionization reactions the reaction rates are taken from BORTNER (1969) when available; otherwise, they are taken from BORTNER (1963). However, one class of dissociation (or association) reactions are taken from BORTNER and BAURER (1972); the positive-ion - neutral dissociation reactions are not considered in the earlier two reaction rate compilations.

Each reaction rate is determined on an individual basis, but generally the guidelines discussed above are used to select the reaction rates. Parameters from BORTNER (1963) and BORTNER (1969) are normalized to 300° K and reaction rates defined in the manner $k_{RR} < 1 \times 10^{-A}$ are re-defined as $k_{RR} = 1 \times 10^{-B}$ where $B = A+1$.
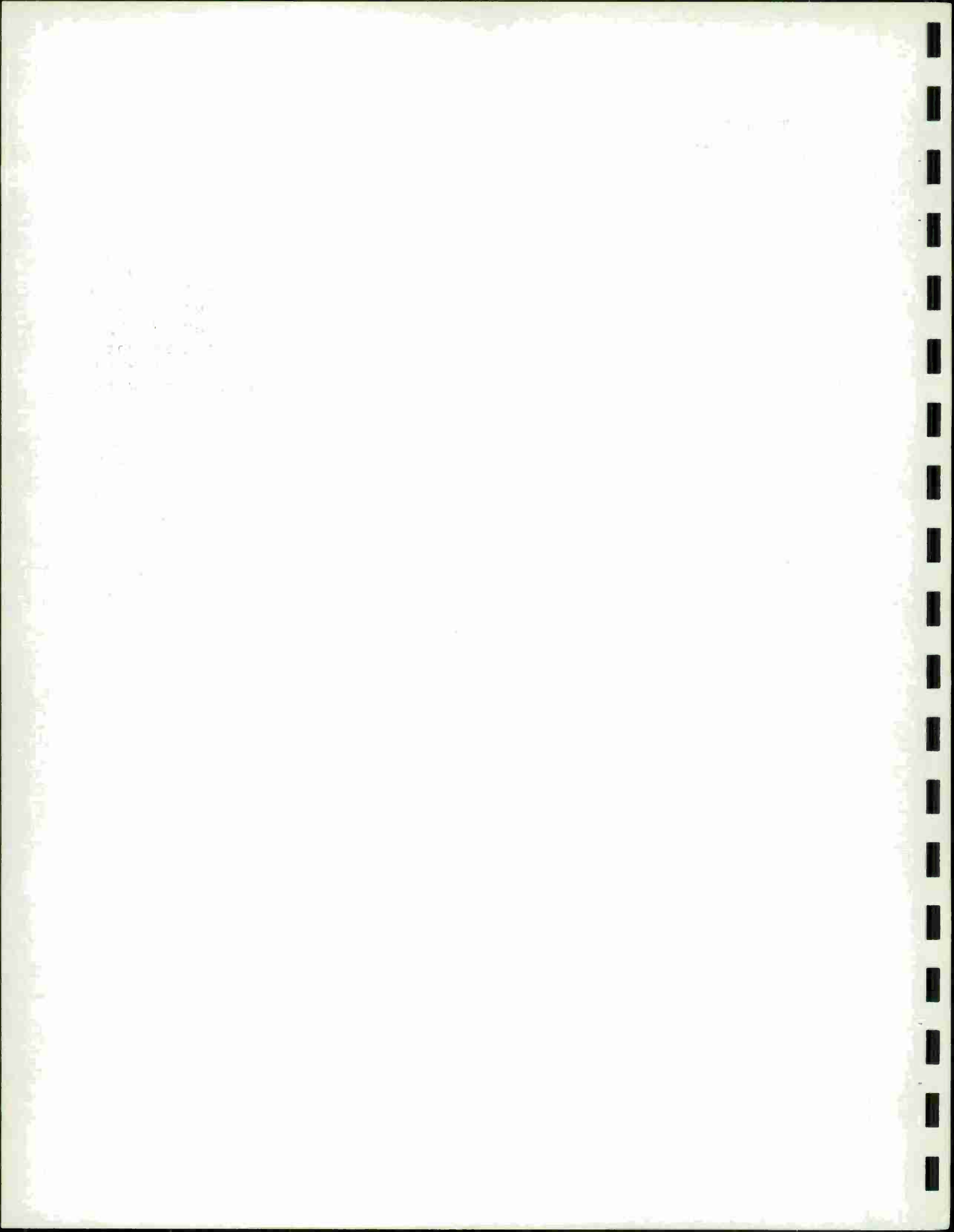
TABLE A-1

REACTIONS AND REACTION RATE CONSTANTS

Dissociation Reactions

Reaction	Reaction Rate	Reference*
$O_2 + O_2 \rightleftharpoons O + O + O_2$	$k_f = 1.2 \times 10^{-7 \pm .5}(T/300)^{-.83}\exp(-59400/T)$	A2
$O_2 + N_2 \rightleftharpoons O + O + N_2$	$k_r = 3.2 \times 10^{-33 \pm .7}(T/300)^{-1.2}$	A2
$O_2 + O \rightleftharpoons O + O + O$	$k_f = 5.0 \times 10^{-7 \pm .7}(T/300)^{-1}\exp(-59400/T)$	A2
$O_2 + X \rightleftharpoons O + O + X$	$k_f = 8.34 \times 10^{-8 \pm .5}(T/300)^{-1.8}\exp(-59400/T)$	A2
$N_2 + N_2 \rightleftharpoons N + N + N_2$	$k_f = 1.15 \times 10^{-7 \pm .5}(T/300)^{-.75}\exp(-113200/T)$	A2
$N_2 + N \rightleftharpoons N + N + N$	$k_f = 9.6 \times 10^{-6 \pm .6}(T/300)^{-1.5}\exp(-113200/T)$	A2

Reaction	Reaction Rate	Reference*
$N_2 + X \rightleftarrows N + N + X$	$k_f = 4.47 \times 10^{-8 \pm .5}(T/300)^{-.82}\exp(-113200/T)$	A2
$NO + N_2 \rightleftarrows N + O + N_2$	$k_r = 1.1 \times 10^{-32 \pm .5}$	A2
$NO + X \rightleftarrows N + O + X$	$k_f = 1.5 \times 10^{-9 \pm .5}\exp(-75400/T)$	A2
$N_2^+ + X \rightleftarrows N^+ + N + X$	$k_r = 1.0 \times 10^{-29 \pm 2}(T/300)^{-1.5 \pm 1.5}$	A3
$O_2^+ + X \rightleftarrows O^+ + O + X$	$k_r = 1.0 \times 10^{-31}$	A3
$NO^+ + X \rightleftarrows N^+ + O + X$	$k_r = 1.0 \times 10^{-29 \pm 2}(T/300)^{-1.5 \pm 1.5}$	A3
$NO^+ + X \rightleftarrows O^+ + N + X$	$k_r = 1.0 \times 10^{-31}$	A3

TABLE A-1   CONTINUED

Rearrangement Reactions

Reaction	Reaction Rate	Reference*
$O + N_2 \rightleftharpoons N + NO$	$k_f = 1.0 \times 10^{-10 \pm .3} \exp(-38000/T)$	A2
$O + NO \rightleftharpoons N + O_2$	$k_f = 3.7 \times 10^{-13 \pm .3} (T/300)^{1.5} \exp(-19100/T)$	A2

Ionization Reactions

Reaction	Reaction Rate	Reference*
$N + O \rightleftarrows NO^+ + e$	$k_r = 4.62 \times 10^{-7\pm.5}(T/300)^{-1.5}$	A2
$N + e \rightleftarrows N^+ + e + e$	$k_r = 4.87 \times 10^{-30\pm1}(T/300)^{-1}$	A1
$N + X \rightleftarrows N^+ + e + X$	$k_r = 3.31 \times 10^{-36\pm2}$	A1
$O + e \rightleftarrows O^+ + e + e$	$k_r = 2.57 \times 10^{-30\pm1}(T/300)^{-1}$	A1
$O + X \rightleftarrows O^+ + e + X$	$k_r = 1.93 \times 10^{-36\pm2}$	A1
$NO + e \rightleftarrows NO^+ + e + e$	$k_r = 1.06 \times 10^{-27\pm1}(T/300)^{-1.5}$	A1
$NO + X \rightleftarrows NO^+ + e + X$	$k_r = 7.96 \times 10^{-34\pm2}(T/300)^{-.5}$	A1
$N + N \rightleftarrows N_2^+ + e$	$k_r = 4.79 \times 10^{-7\pm1}(T/300)^{-.5}$	A1

Ionization Reactions

Reaction	Reaction Rate	Reference*
$O + O \;\rightleftharpoons\; O_2^+ + e$	$k_r = 2.77 \times 10^{-7\pm1}(T/300)^{-1}$	A1
$N_2 + N_2 \rightleftharpoons N_2^+ + e + N_2$	$k_r = 5.2 \times 10^{-35\pm2}(T/300)^{.5}$	A2
$N_2 + e \rightleftharpoons N_2^+ + e + e$	$k_r = 1.77 \times 10^{-29\pm1}(T/300)^{-1}$	A2
$N_2 + X \;\rightleftharpoons\; N_2^+ + e + X$	$k_r = 3.58 \times 10^{-38\pm2}(T/300)^{1.5}$	A1
$O_2 + N_2 \rightleftharpoons O_2^+ + e + N_2$	$k_r = 1.6 \times 10^{-36\pm2}$	A2
$O_2 + O_2 \rightleftharpoons O_2^+ + e + O_2$	$k_r = 3.2 \times 10^{-36\pm2}$	A2
$O_2 + e \;\rightleftharpoons\; O_2^+ + e + e$	$k_r = 1.17 \times 10^{-29\pm1}(T/300)^{-1}$	A2
$O_2 + X \;\rightleftharpoons\; O_2^+ + e + X$	$k_r = 1.37 \times 10^{-35\pm2}(T/300)^{-.5}$	A1

Positive-Ion Charge Exchange

Reaction	Reaction Rate	Reference*
$N^+ + O \rightleftarrows N + O^+$	$k_f = 1.0 \times 10^{-12}(T/300)^{\pm 1.5}$	A3
$N^+ + O_2 \rightleftarrows NO^+ + O$	$k_f = 3.0 \times 10^{-10}(T/300)^{\pm 1.5}$	A3
$N^+ + NO \rightleftarrows N + NO^+$	$k_f = (8 \pm 2.4) \times 10^{-10}(T/300)^{\pm 1.5}$	A3
$O^+ + N_2 \rightleftarrows NO^+ + N$	$k_f = 1.2 \times 10^{-12}(T/300)^{0.5}$	A3
$O^+ + NO \rightleftarrows O + NO^+$	$k_f = 1.3 \times 10^{-13}(T/300)^{\pm 1.5}$	A3
$N_2^+ + N \rightleftarrows N + N^+$	$k_f = 1.0 \times 10^{-12}(T/300)^{\pm 1.5}$	A3
$N_2^+ + O \rightleftarrows N_2 + O^+$	$k_f = 6.0 \times 10^{-12}(T/300)^{\pm 1.5}$	A3
$N_2^+ + O \rightleftarrows NO^+ + N$	$k_f = 2.5 \times 10^{-10 \pm .7}(T/300)^{\pm 1.5}$	A2

Positive-Ion Charge Exchange

Reaction	Reaction Rate	Reference*
$N_2^+ + O_2 \rightleftarrows N_2 + O_2^+$	$k_f = 1.0 \times 10^{-10 \pm .3}(T/300)^{\pm 1.5}$	A2
$N_2^+ + O_2 \rightleftarrows NO^+ + NO$	$k_f = 1.0 \times 10^{-17 \pm 2}(T/300)^{\pm 1.5}$	A2
$N_2^+ + NO \rightleftarrows N_2 + NO^+$	$k_f = 5.0 \times 10^{-10 \pm .3}(T/300)^{\pm 1.5}$	A2
$N^+ + O_2 \rightleftarrows N + O_2^+$	$k_f = (3.0 \pm 1.5) \times 10^{-10}(T/300)^{\pm 1.5}$	A3
$O^+ + O_2 \rightleftarrows O + O_2^+$	$k_f = 2.0 \times 10^{-11}(T/300)^{-.5}$	A3
$O^+ + NO \rightleftarrows O_2^+ + N$	$k_f = 1.0 \times 10^{-13}(T/300)^{\pm 1.5}$	A3
$O_2^+ + N_2 \rightleftarrows NO^+ + NO$	$k_f = 1.0 \times 10^{-16 {}^{+1}_{-3}}(T/300)^{\pm 1.5}$	A3
$O_2^+ + N \rightleftarrows NO^+ + O$	$k_f = (1.8 \pm .6) \times 10^{-10}(T/300)^{\pm 1.5}$	A3

Positive-Ion Charge Exchange

Reaction	Reaction Rate	Reference*
$O_2^+ + NO \rightleftharpoons O_2 + NO^+$	$k_f = (6.3 \pm 2.4) \times 10^{-10} (T/300)^{\pm 1.5}$	A3
$NO^+ + N + X \rightleftharpoons O^+ + N_2 + X$	$k_r = 2.8 \times 10^{-28} (T/300)^{-1.5 \pm 1.5}$	A3
$NO^+ + O + X \rightleftharpoons O^+ + NO + X$	$k_r = 1.0 \times 10^{-29 \pm 2} (T/300)^{-1.5 \pm 1.5}$	A3

---

*Reference Notation: A1 - BORTNER (1963), A2 - BORTNER (1968), A3 - BORTNER and BAURER (1972).

APPENDIX B: VIBRATIONAL RELAXATION EQUATION

The relaxation equation for vibrational energy is presented below*

$$\frac{dE_v}{dx} = \frac{(E_v)_{VIB.\ EQ.} - E_v}{\tau_p\ (U - u)}$$

$$- \left(\frac{k\Theta_v}{(e^{\Theta_v/T_{m}}-1)} - \frac{(N+1)k\Theta_v}{(e^{(N+1)\Theta_v/T_{m}}-1)} - E_v \right) \frac{1}{(X)} \left(\frac{d(X)}{dx} \right)_{DISS}$$

$$+ (\frac{1}{2}\ k\Theta_v\ N - E_v)\ \frac{1}{(X)} \left(\frac{d(X)}{dx} \right)_{REC}$$

$$- \frac{Q_3}{(X_{N_2})nu}$$

There is a separate equation for each species which undergoes vibrational relaxation. Vibrational relaxation is considered for two species in this model, O_2 and N_2. The other molecular species are assumed to be formed in vibrational-translational equilibrium.

The first term in the above equation considers collisional-vibrational energy exchange. Values for characteristic relaxation times, τ, are taken from MILLIKAN and WHITE (1963). The simple harmonic oscillator model is used for computing the vibrational energy as a function of either the local translational temperature $(E_v)_{VIB.\ EQ.}$ (T) or the local vibrational temperature $E_v\ (T_v)$.

The middle two terms correct the vibrational relaxation rate by including the effects of the dissociation process (TREANOR and MARRONE (1962)). The more energetic vibrators are more easily dissociated. This process lowers the average vibrational energy in the molecules that remain. However, the assumption that dissociation does not perturb the Boltzmann distribution is maintained. An additional correction is included to take into account the change in the number of oscillators during the dissociation process.

The last term in the relaxation equation considers electron-vibrational energy exchange which only applies to N_2 and will be discussed in connection with the electron energy equation.

---

*See 6. LIST OF SYMBOLS of text.
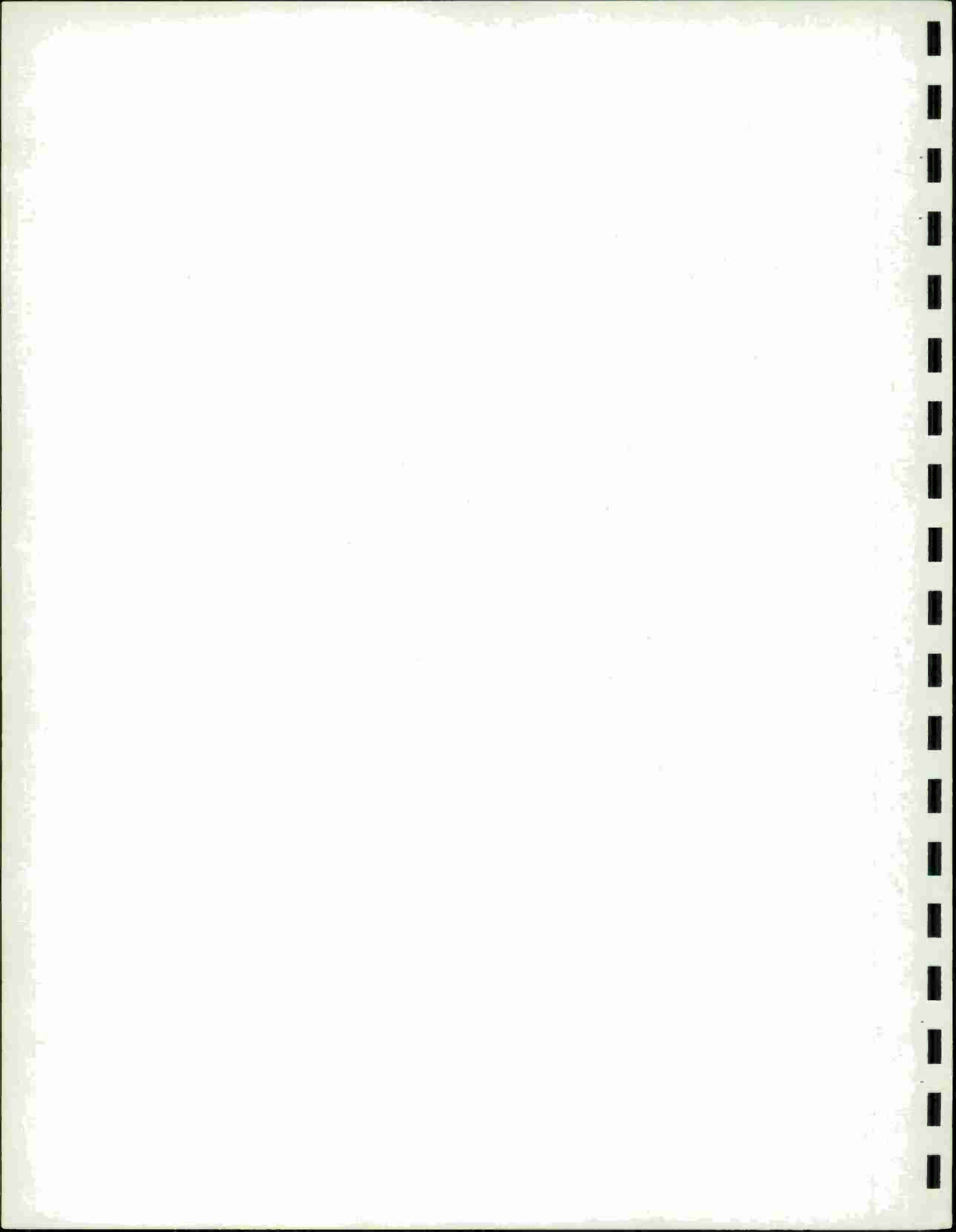
APPENDIX C: ELECTRON ENERGY EQUATION

The form of the electron energy equation used is*

$$\frac{dT_e}{dx} = \frac{\sum\limits_1^5 Q_i}{\frac{3}{2}n_e uk} - \frac{T_e}{n_e}\frac{dn_e}{dx} \, ,$$

with the following electron energy flux terms.

$$Q_1 = \sum_i (6.853 \times 10^{-43})\frac{(T-T_e)}{m_i T_e^{3/2}} \, (\ell n((7.675 \times 10^7) \frac{T_e^3}{n_e}) + 1.0)(X)_i(X_e)n^2 .$$

Q_1 is the energy gained by electrons through elastic collisions with ions (BIBERMAN and YAKUBOV (1965)). Summation is over all ions i in the air chemistry model. Electron-neutral elastic collision energy exchange is negligible in comparison and is not included.

$$Q_2 = -\sum_i E_{I_i} (D_{ea})_i n^2 \, .$$

Q_2 is the energy lost by electrons through electron-neutral collisional ionization reactions. $(D_{ea})_i$ is the net production rate (CM^3/SEC), forward minus reverse, for the ith electron-neutral collisional ionization reaction and E_{I_i} is the corresponding ionization energy; i is summed over the electron-neutral collisional ionization reactions in the air chemistry model.

$$Q_3 = (4.5 \times 10^{-9}) e^{-10^4/T_e} k\theta_{v_{N_2}} (e(TVN2)-e(T_e))(e(TVN2)+e(T_e)+1)$$

$$\cdot (X_e)(X_{N_2})n^2,$$

where

$$e(T) = \left(e^{(\Theta_v)_{N_2}/T} -1\right)^{-1} \, .$$

---

*See 6. LIST OF SYMBOLS of text.

Q_3 is the energy gained by electrons through collisions with N_2 molecular oscillators (BIBERMAN, MNATSAKANYAN, and YAKUBOV (1971)). In general, the direct excitation of vibrational levels of diatomic molecules by collision with slow electrons is not efficient because of the differences in masses of the collision partners. However, for N_2 the slow electron is captured forming an unstable negative ion. Following the decay, the final vibrational quantum number may be several steps above the initial quantum number which effects a considerable change in the electron energy. This mechanism also applies to CO which is not included in the present air-chemistry model. Q_3 is in the N_2 vibrational relaxation equation.

$$Q_4 = \frac{3}{2} kT(k_{AI})_f \, n^2 - \frac{3}{2} kT_e (k_{AI})_r \, n^2 \quad .$$

Q_4 is the energy gained by electrons from associative ionization reactions (ZHELEZNYAK and MNATSAKANYAN (1968)). $(k_{AI})_f$ and $(k_{AI})_r$ are the net forward and reverse reaction rates (CM^3/SEC) for associative ionization summed over reactions in the air chemistry model.

$$Q_5 = -n^2 (Xe) \, P_e(T_e) \, (E_O X_O + E_N X_N + E_O \, X_O + E_{O^+} X_O + E_{N^+} X_{N^+}$$

$$+ \, E_{O_2^+} X_{O_2^+} + E_{N_2^+} X_{N_2^+}) \ ,$$

where $P_e(T_e) = a_e v_e = 6.212 \times 10^{-12} \, T_e^{1/2}.$*

Q_5 is the energy lost by electrons maintaining the quasistationary population of excited states. The electron excitation energies for species N_2, NO, and NO^+ are negligible in comparison with contributions from the other species.

---

*An approximate value of $a_e = 10^{-17} CM^2$ was selected (ZEL'DOVICH and RAIZER (1966)).

APPENDIX D: ENTHALPY EQUATION

Enthalpy is defined as*

$$h(T, T_v, T_e, X_i) = \frac{5}{2}(1-X_e)RT + \frac{5}{2}X_e R T_e$$

$$+ \sum_j X_j \left(\frac{R(\Theta_v)_j}{e^{(\Theta_v)_j/T_{v_j}}} + RT \right)$$

$$+ \sum_\ell X_\ell \left(\frac{\sum_i (g_i/g_o)_\ell (\Theta_i)_\ell e^{-(\Theta_i)_\ell/T_e}}{1 + \sum_i (g_i/g_o)_\ell e^{-(\Theta_i)_\ell/T_e}} + (h_F)_\ell \right) .$$

The summations are given to be: j - molecules and molecular ions, ℓ - all chemical species, i - electronic levels. The vibrational model used is the harmonic oscillator. Separate vibrational temperatures are considered for O_2 and N_2 vibrators whereas all other species are evaluated at the translational temperature. All rotational energy modes are assumed to be excited at the classical limit in equilibrium with translation, and the distribution of electronic states corresponds to the free electron temperature; that is, the bound and free electrons are in equilibrium. The thermodynamic constants are taken from BORTNER and BAURER (1972).

---

*See 6. LIST OF SYMBOLS of text.
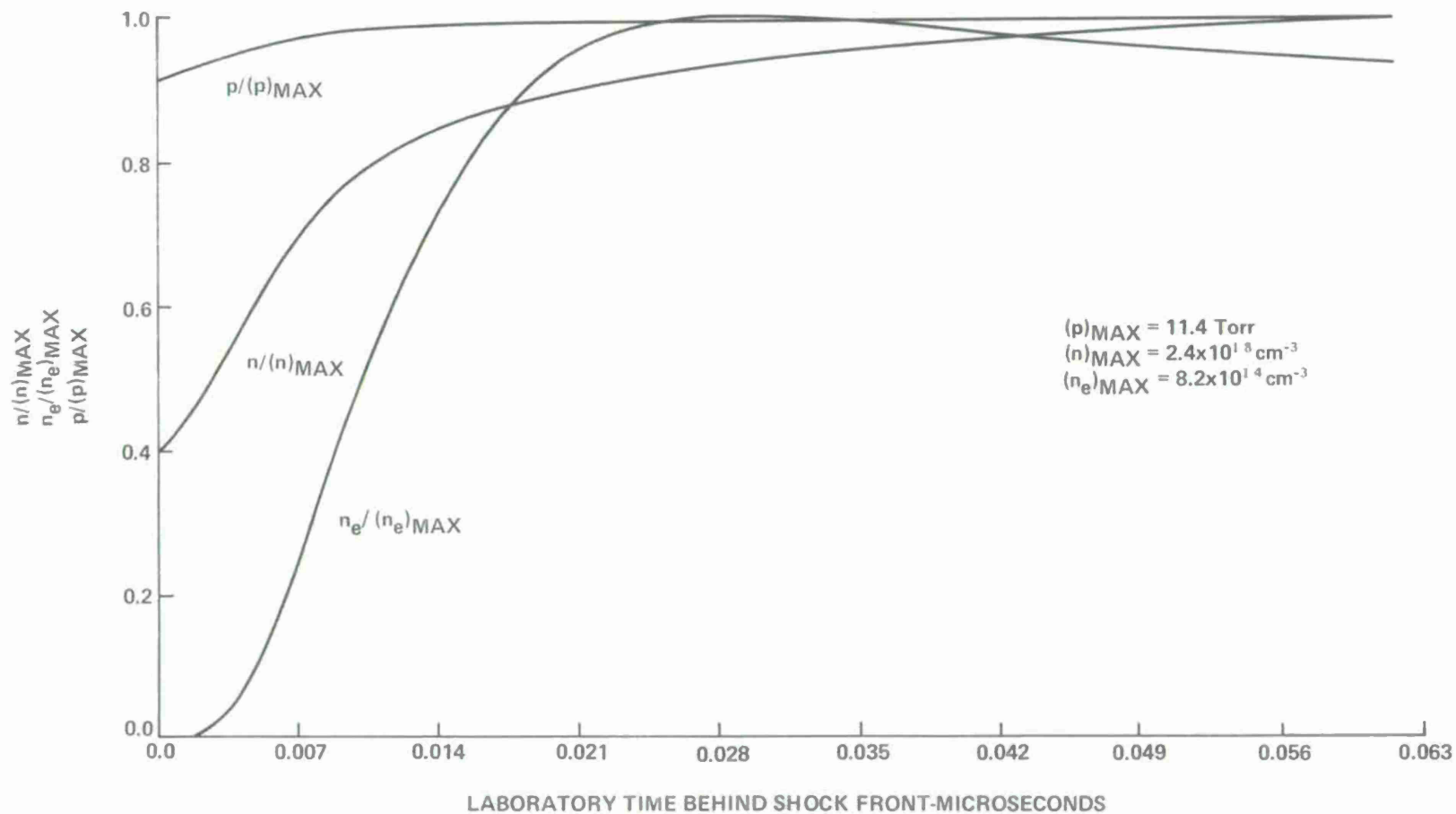
FIG. 1. TOTAL NUMBER DENSITY, ELECTRON NUMBER DENSITY, AND PRESSURE PROFILES IN RELAXATION REGION FOR M = 16.47, p = 5 TORR, T = 300° K
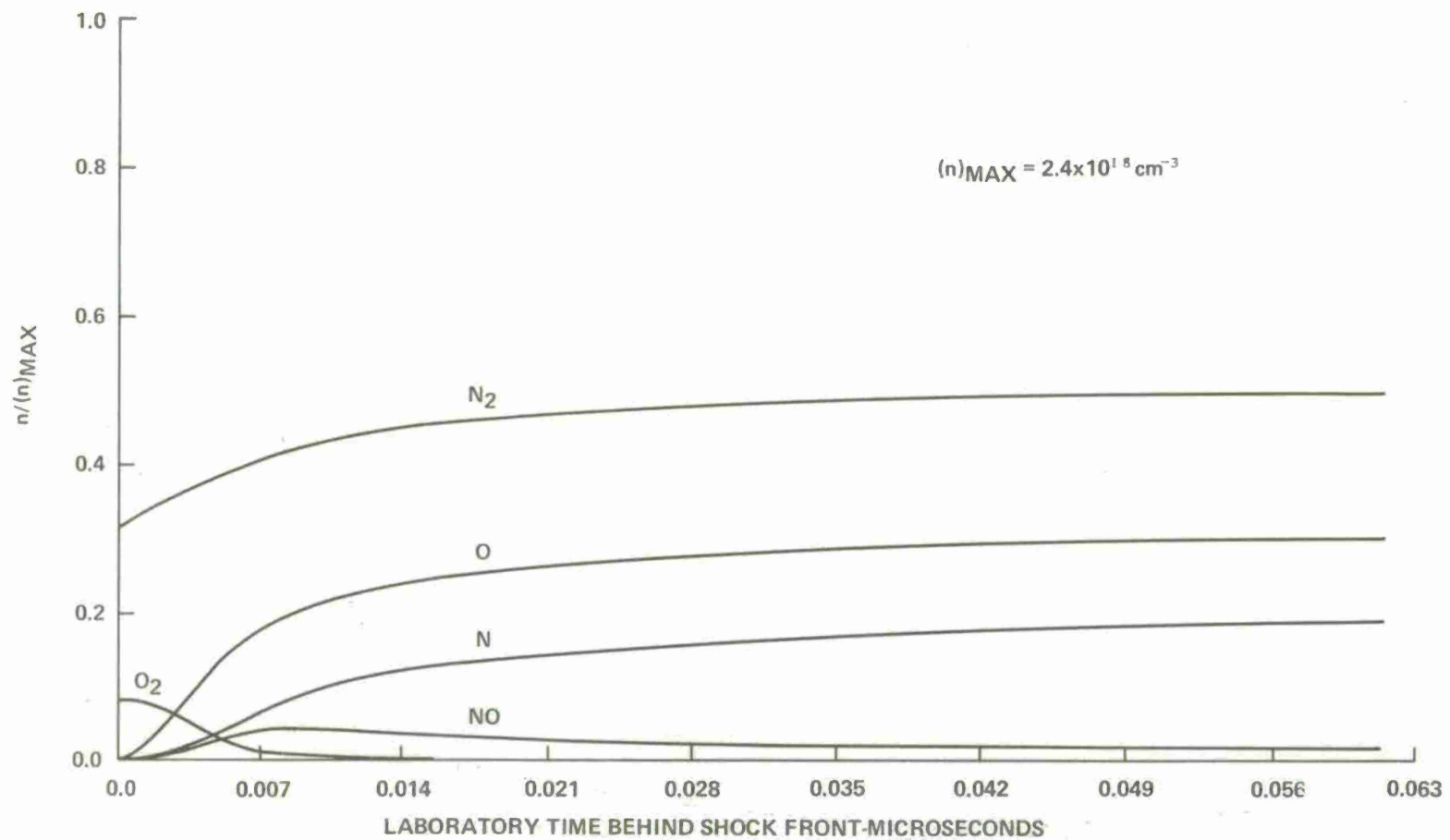
FIG. 2. NEUTRAL SPECIES(O_2, N_2, NO, O, N) PROFILES IN RELAXATION REGION FOR M = 16.47, p = 5 TORR, T = 300° K
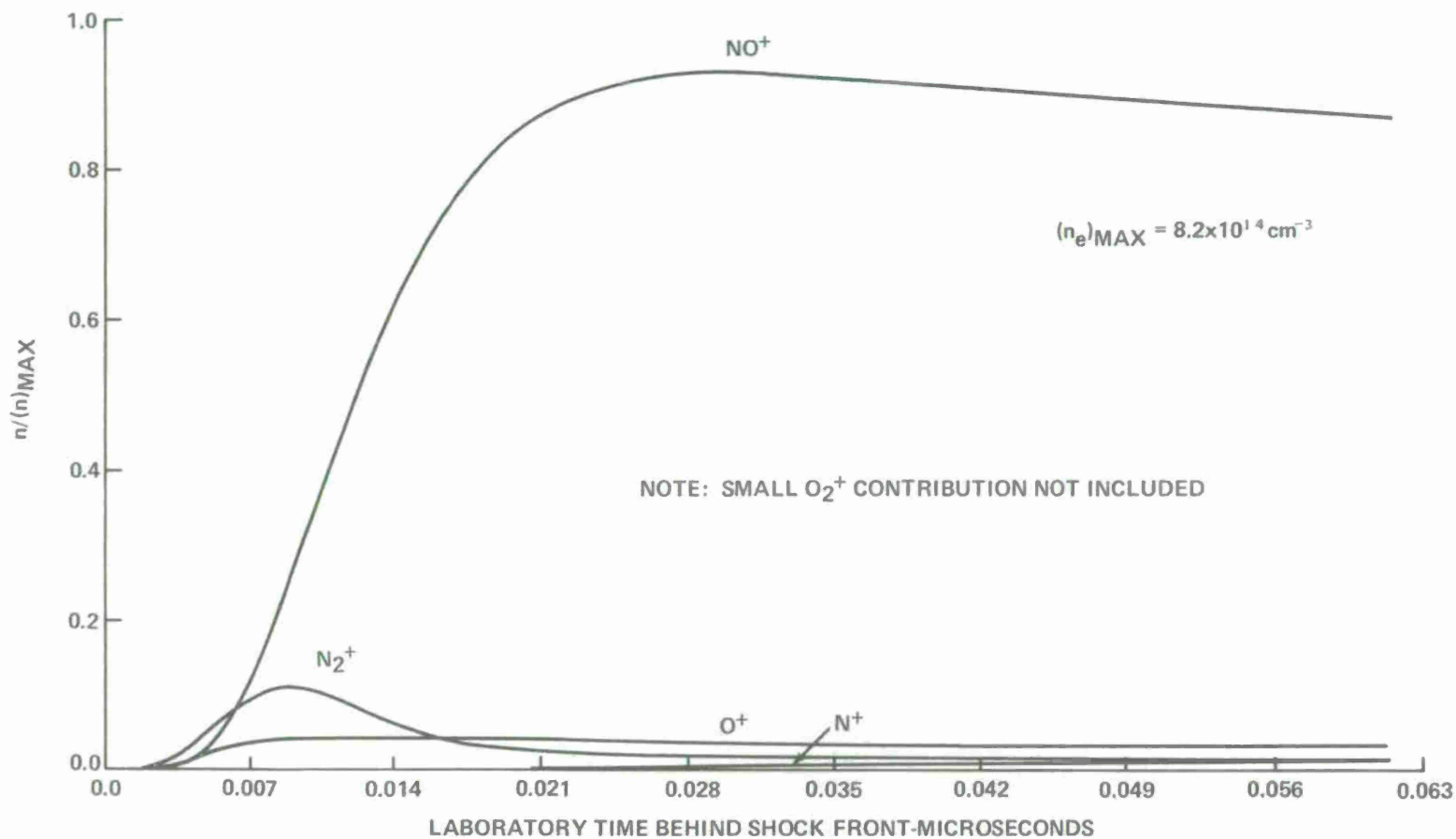
FIG. 3. CHARGED SPECIES (N_2^+, NO^+, O^+, N^+) PROFILES IN RELAXATION REGION FOR
M = 16.47, p = 5 TORR, T = 300°K
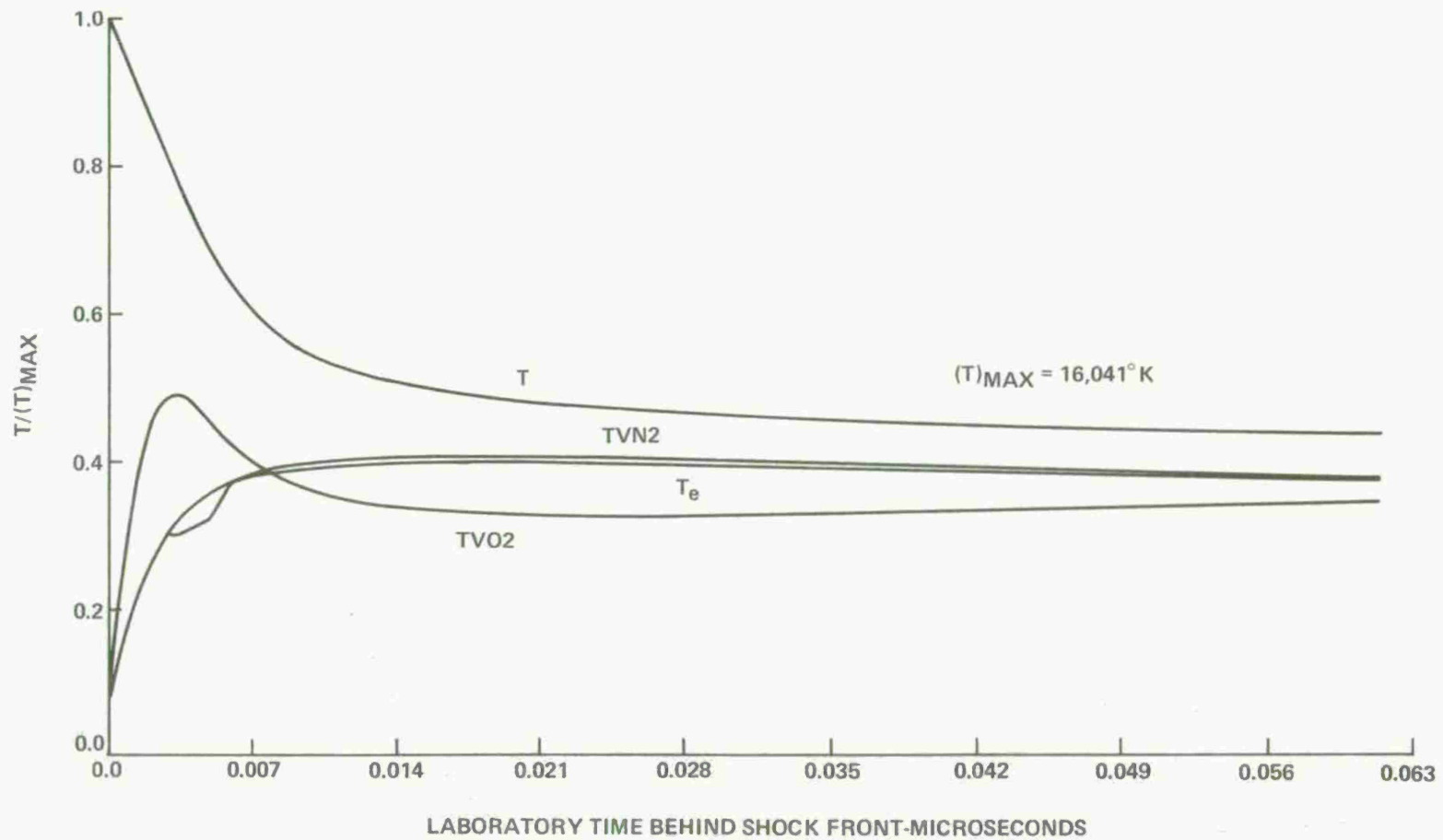
FIG. 4. TEMPERATURE (TRANSLATION, ELECTRON, O_2 VIBRATION, N_2 VIBRATION) PROFILES IN
RELAXATION REGION FOR M = 16.47, p = 5 TORR, T = 300°K
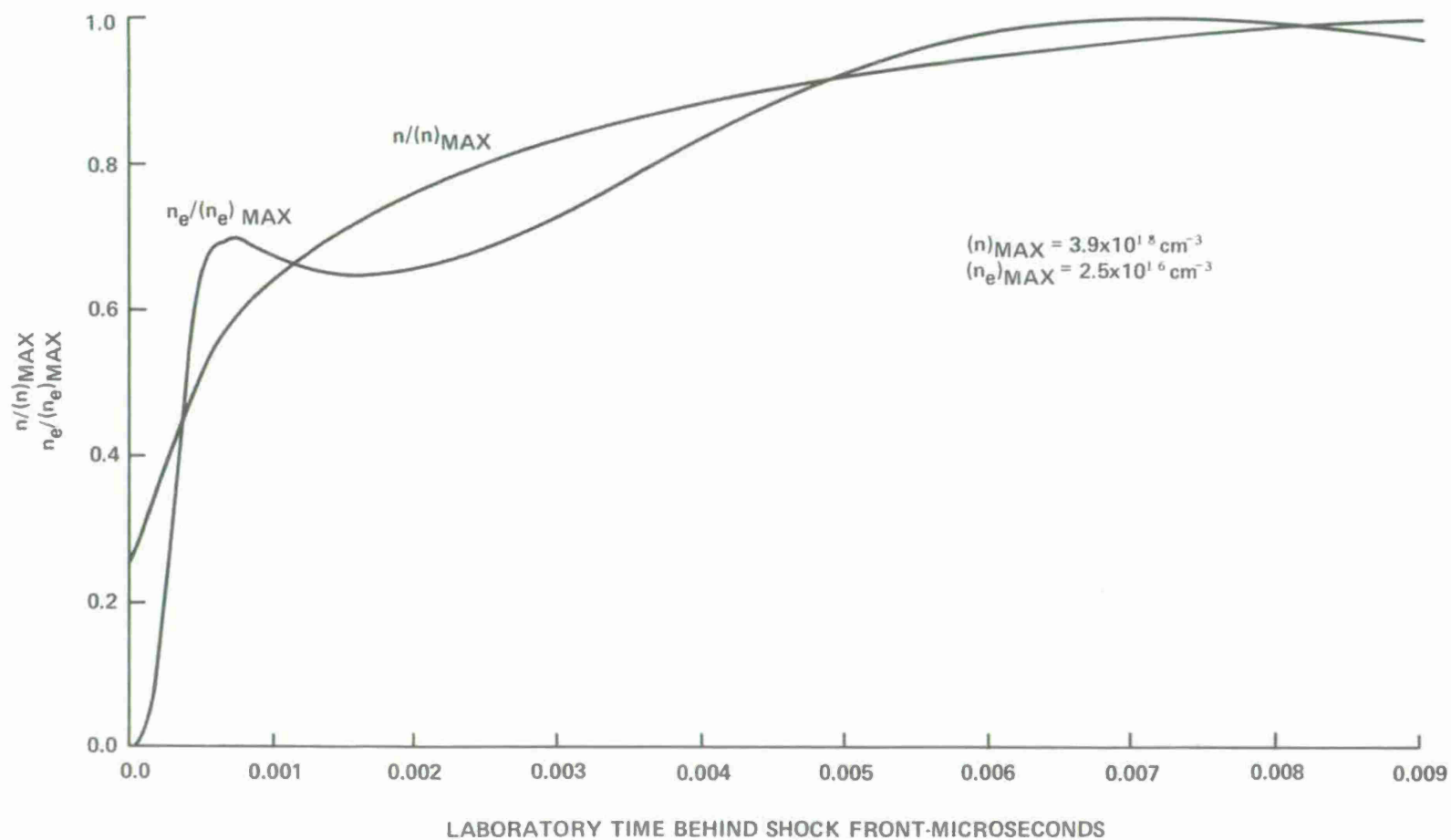
FIG. 5. TOTAL NUMBER DENSITY AND ELECTRON NUMBER DENSITY PROFILES IN RELAXATION REGION FOR M = 26.76, p = 5 TORR, T = 300° K
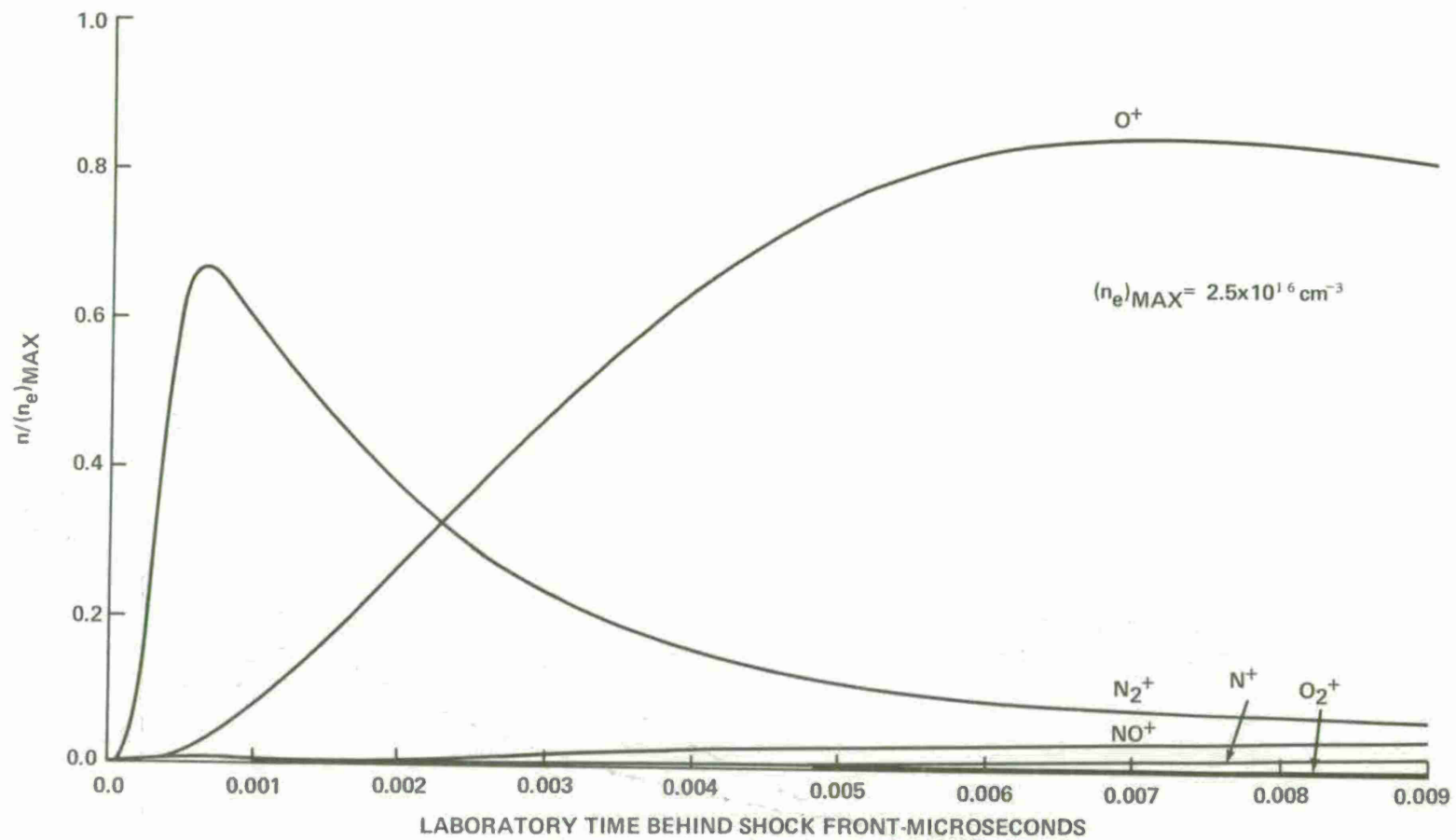
FIG. 6. CHARGED SPECIES (O_2^+, N_2^+, NO^+, O^+, N^+) PROFILES IN RELAXATION REGION FOR
M = 26.76, p = 5 TORR, T = 300° K
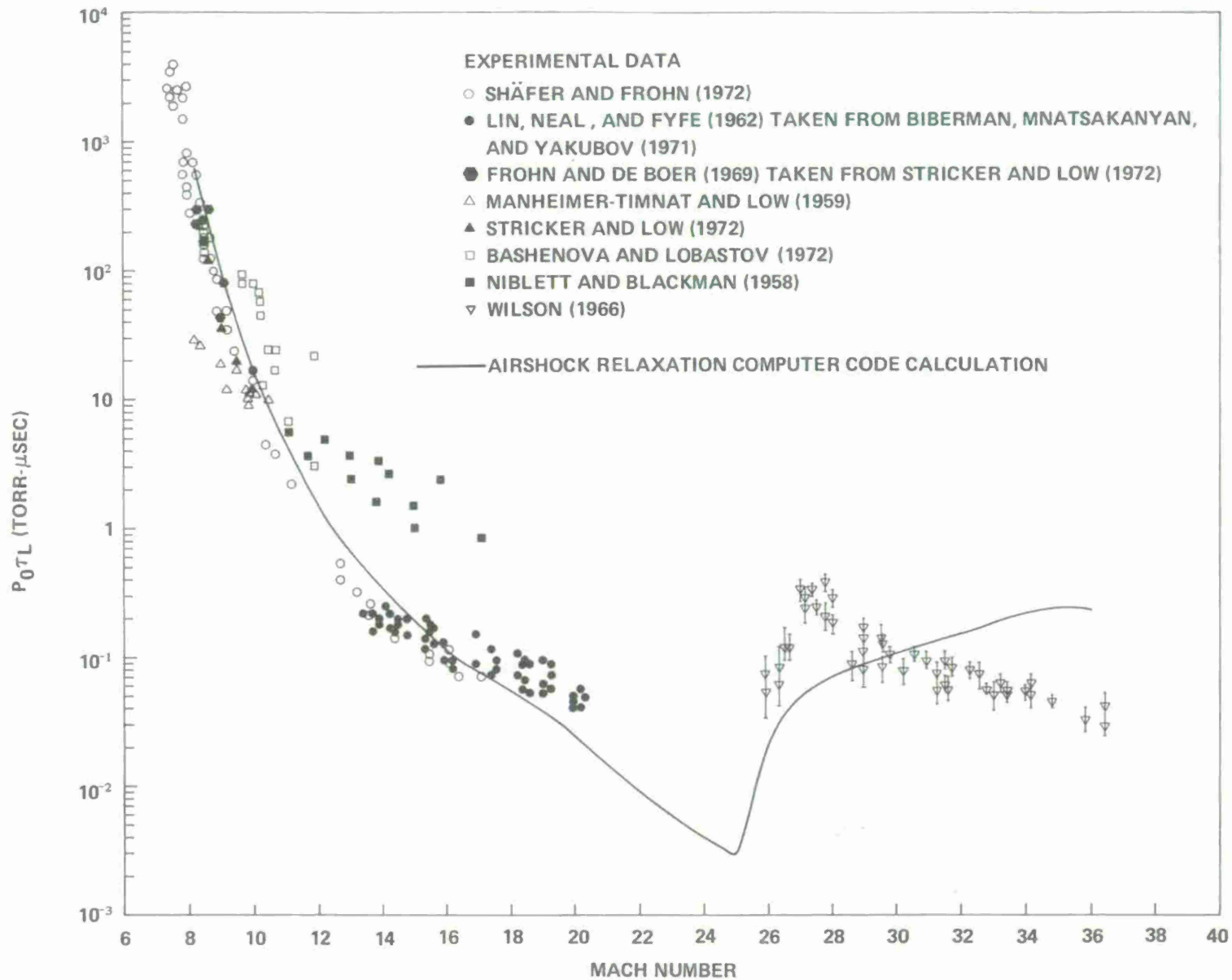
FIG. 7 DEPENDENCE ON MACH NUMBER OF THE PRODUCT OF IONIZATION RELAXATION
TIME IN LABORATORY COORDINATES AND UPSTREAM AMBIENT PRESSURE IN AIR
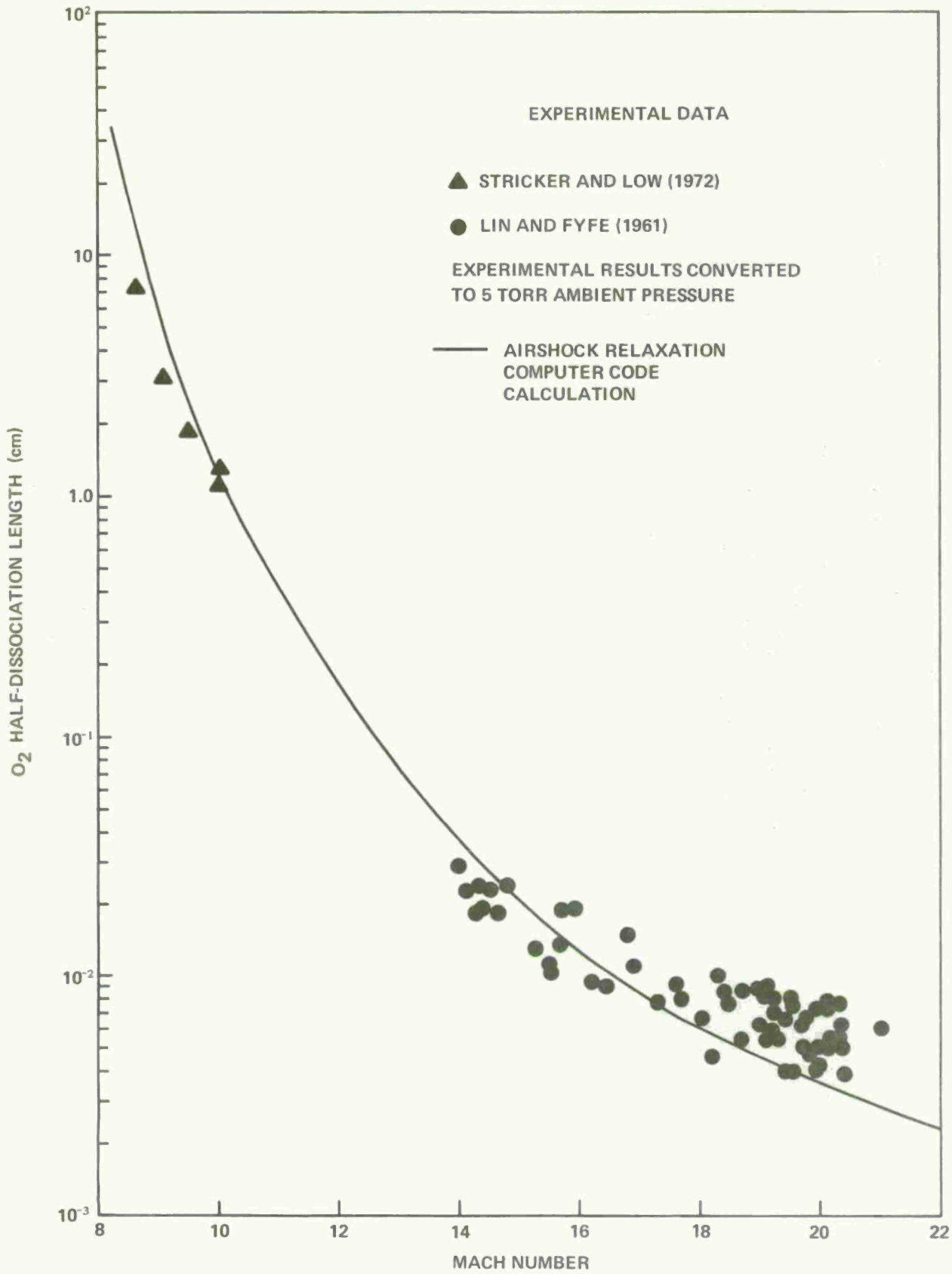
FIG. 8. DEPENDENCE ON MACH NUMBER OF O_2 HALF-DISSOCIATION LENGTH IN AIR
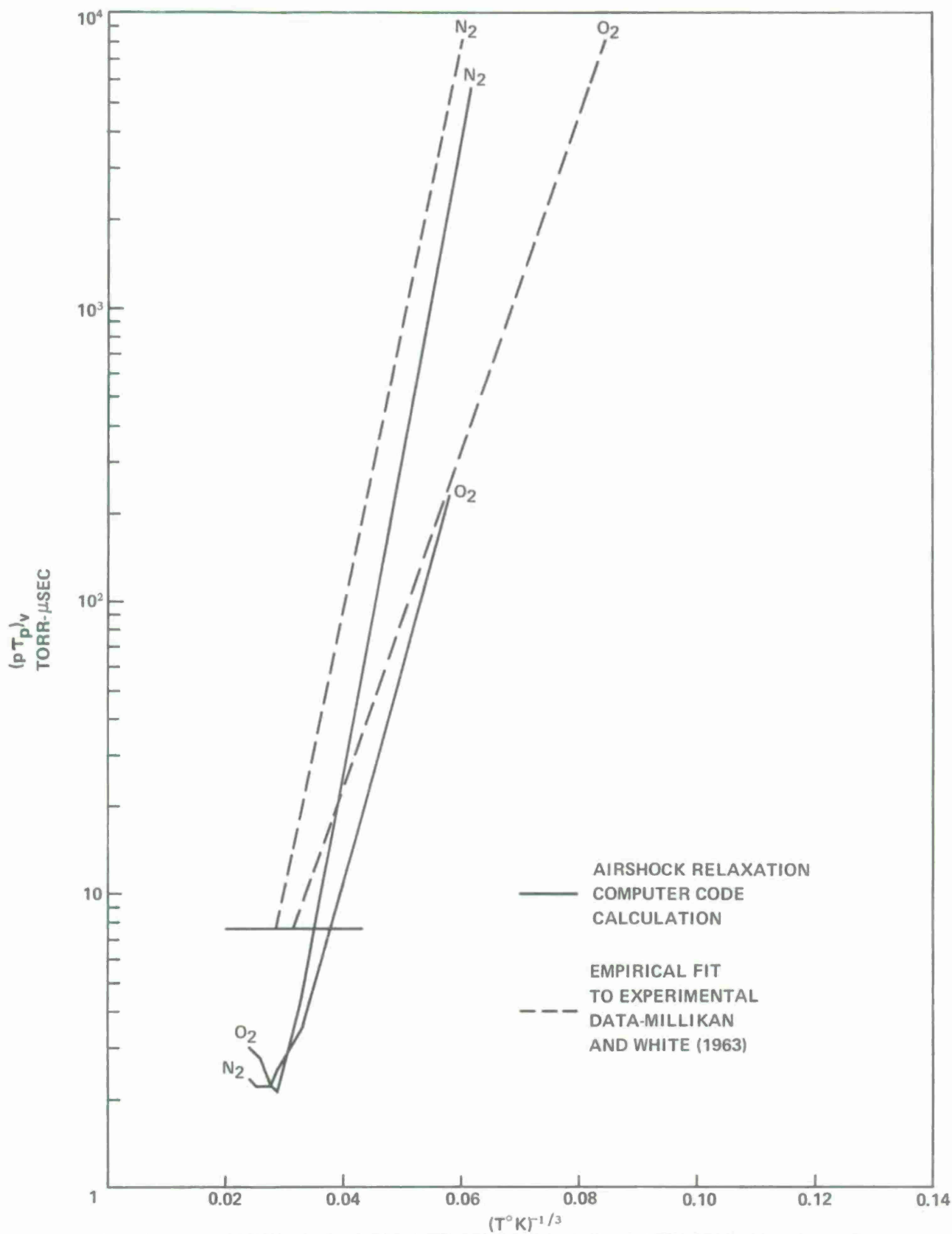
FIG. 9. DEPENDENCE ON TEMPERATURE OF THE PRODUCT OF VIBRATIONAL RELAXATION TIME IN PARTICLE COORDINATES AND DOWNSTREAM PRESSURE FOR O_2 AND N_2

DISTRIBUTION   <u>Copies</u>
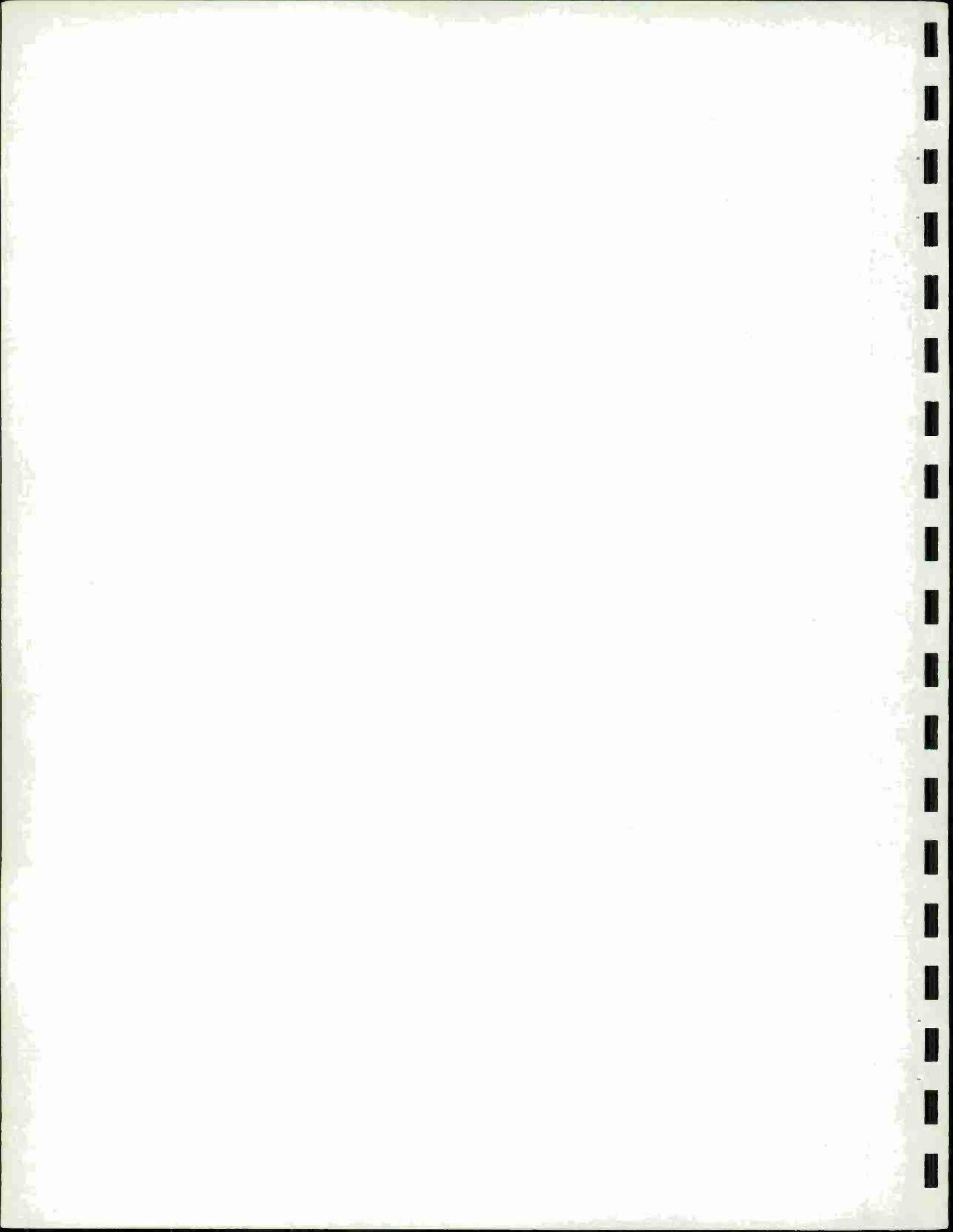
Chief of Naval Material
Naval Material Command Hdqtrs
Department of the Navy
Washington, D. C. 20360
  Attn: Code 03L

Commander
Naval Ship Engineering Center
Prince George's Center
Hyattsville, MD 20782
  Attn: 6105G, R. Fuss
        6105G, D. Hurt

Commander
Naval Air Systems Command
Washington, D. C. 20360
  Attn: AIR-350
        AIR-53233C

Commander
Naval Sea Systems Command
Washington, D. C. 20361
  Attn: SEA-033
        SEA 03511, C. Pohler

Chief of Naval Research
Washington, D. C. 20390
  Attn: Code 418, Gracen Joiner

President
Naval War College
Newport, R.I. 02840

Superintendent
Naval Postgraduate School
Monterey, CA 93940
  Attn: Prof. Otto Heinz, Dept of Physics
        Prof. E. A. Milne

Commander
Naval Weapons Center
China Lake, CA 93555
  Attn: Library, R. E. Boyer
                 D. Mallory

Commander
Naval Ship Research and Development Center
Bethesda, MD 20034
  Attn: Library

Commanding Officer
Naval Weapons Evaluation Facility
Kirtland AFB, Albuquerque, NM 87117
  Attn: Library

Copies

Commanding Officer
Naval Ordnance Station
Indian Head, MD 20640
  Attn: Technical Library

Commander
Naval Surface Weapons Center
Dahlgren, VA 22448
  Attn: Technical Library

Commanding Officer
U. S. Army Combat Developments Command
Institute of Nuclear Studies
Fort Bliss, TX 79916

Director
U. S. Army Ballistic Research Laboratories
Aberdeen Proving Ground, MD 21005
  Technical Library
  AMXBR-X, R. J. Eichelberger
  AMXBR-VL, A. J. Hoffman
  AMXBR-DL, B. P. Bertrand
  AMXBR-TB, C. N. Kingery
  AMXBR-TB, W. J. Taylor

Commanding Officer
Picatinny Arsenal
Dover, NJ 07801
  Attn: Technical Library
        SARPA-TS-S #59

Director
U. S. Army Engineers
Waterways Experiment Station
Vicksburg, MS 39180
  Attn: Technical Library

Commanding Officer
Harry Diamond Laboratories
Connecticut Ave and Van Ness St., N.W.
Washington, D. C. 20438
  Attn: Library

Flight Dynamics Laboratory
Wright-Patterson AFB, OH 45433

AF Cambrdige Research Laboratory
Hanscom Field
Bedford, MA 01731
  Attn: Dr. N. Rosenberg

Copies

Director
Air University Library
Maxwell AFB, AL 36112

Commander
Air Force Office of Scientific Research
1400 Wilson Blvd
Arlington, VA 22209
   Attn: Library

Air Force Weapons Laboratory, AFSC
Kirtland AFB, NM 87117
   Attn: CAPT D. Matuska

Director of Defense Research and Engineering
Washington, D. C. 20330
   Attn: Technical Library

Director
Weapons Systems Evaluation Group, OSD
Room 1E880
The Pentagon
Washington, D. C. 20301

Commandant
Armed Forces Staff College
Norfolk, VA 23500
   Attn: Library

Commander
Test Command, Defense Nuclear Agency
Sandia Base
Albuquerque, NM 87115
   Attn: FCWT, FCTG

Director
Defense Nuclear Agency
Washington, D.C. 20305
   Attn: Dr. C. Blank
        J. Kelso
        J. F. Moulton, Jr.
        LT R. Williams

Los Alamos Scientific Laboratory
University of California
P.O. Box 1663
Los Alamos, New Mexico 87544
   Attn: Dr. J. Zinn
        Dr. H. Hoerlin
        Dr. J. Kodis
        Technical Library

Copies

NASA Scientific and Technical Information Facility
P. O. Box 33
College Park, MD 20740

Chief
Classified Technical Library
Technical Information Service
U. S. Atomic Energy Commission
Washington, D. C. 20545
    Attn: Technical Library

President
Sandia Laboratories
Albuquerque, NM 87115
    Attn: J. W. Reed, Div. 5644

E. O. Lawrence Radiation Laboratory
University of California
P. O. Box 808
Livermore, CA 94550
    Attn: Technical Information Div.
          Dr. Joseph B. Knox
          Dr. E. C. Woodward

National Aeronautics and Space Administration
Manned-Spacecraft Center
Space Technology Division
Box 1537
Houston, TX 77058
    Attn: Mr. R. F. Fletcher

Director
U. S. Bureau of Mines
Division of Explosive Technology
4800 Forbes Street
Pittsburgh, PA 15213
    Attn: Dr. Robert W. Van Dolah

Civil Defense Research Project
Oak Ridge National Laboratory
P. O. Box X
Oak Ridge, TN 37830
    Attn: Dr. Carsten Haaland

President (DA-49-146-XZ-458)
Kaman Nuclear
Colorado Springs, CO 80900
    Attn: Mr. P. Wells
          Dr. D. Sachs

Copies

Denver Research Institute (N60921-7145)
Mechanics Division, University of Denver
Denver, CO 80210
    Attn: Mr. J. Wisotski
    Via: ONRRR, Lawrence, KS 66044

Director (Now 66-0161-d)
New Mexico Institute of Mining Technology
Socorro, New Mexico 87801
    Attn: Dr. M. Kempton

Director (Now 65-0207-d)
Applied Physics Laboratory
Johns Hopkins University
8621 Georgia Avenue
Silver Spring, MD 20910
    Attn: Technical Library

Physics International Company
2229 4th Street
Berkeley, CA 94710
    Attn: Technical Library

DDC   12
Cameron Station
Alexandria, VA 22314
    Attn: TISIA-21

Falcon Research and Development (N123(60530)50031A)
1441 Ogden Street
Denver, CO 80218
    Attn: Mr. D. K. Parks

Space Sciences Laboratory (N60921-7164)
General Electric Company
P. O. Box 8555
Philadelphia, PA 19101
    Attn: Dr. S. M. Scala
          Dr. M. H. Bortner

National Research Council
Commission on Human Relations
Associatship Office, Dr. H. W. Lucien
2101 Constitution Ave
Washington, D. C. 20418

Institute for Defense Analyses
400 Army Navy Drive
Arlington, VA 22202
    Attn: Library
          E. Bauer

Copies

AVCO-Everett Research Laboratory
2385 Revere Beach Parkway
Everett, MA 02149
   Attn: J. Wilson

AVCO Systems Division
201 Lowell St
Wilmington, MA 01887
   Attn: R. E. Cooper

Southwest Research Institute
8500 Culebra Road
San Antonio, TX 78228
   Attn: Dr. W. E. Baker

Technical Information Service
American Institute of Aeronautics and
  Astronautics
750 Third Avenue
New York, NY 10017

R&D Associates
P. O. Box 3580
Santa Monica, CA 90403
   Attn: H. L. Borde

TO AID IN UPDATING THE DISTRIBUTION LIST
FOR NOL TECHNICAL REPORTS PLEASE COMPLETE
THE FORM BELOW

TO ALL HOLDERS OF __NOLTR 74-182__
by Jerry M. Ward, Code 241

DO NOT RETURN THIS FORM IF ALL INFORMATION IS CURRENT

A. FACILITY NAME AND ADDRESS *(OLD) (Show Zip Code)*

NEW ADDRESS *(Show Zip Code)*

B. ATTENTION LINE ADDRESSES:

C.

☐ REMOVE THIS FACILITY FROM THE DISTRIBUTION LIST FOR TECHNICAL REPORTS ON THIS SUBJECT.

D.

NUMBER OF COPIES DESIRED _____

GPO 878-354